2-P

X-690-72-337
PREPRINT

NASA TM X- 66023

COMETARY EXPLORER TO GRIGG-SKJELLERUP 1977

SEPTEMBER 1972

N. F. NESS
L. F. BURLAGA
R. W. FARQUHAR
B. D. DONN
W. M. JACKSON
D. K McCARTHY

GSFC — GODDARD SPACE FLIGHT CENTER
GREENBELT, MARYLAND

X-690-72-337

COMETARY EXPLORER TO

GRIGG-SKJELLERUP 1977

N. F. Ness
L. F. Burlaga
R. W. Farquhar
B. D. Donn
W. M. Jackson
D. K. McCarthy

Goddard Space Flight Center
Greenbelt, Maryland

September 1972

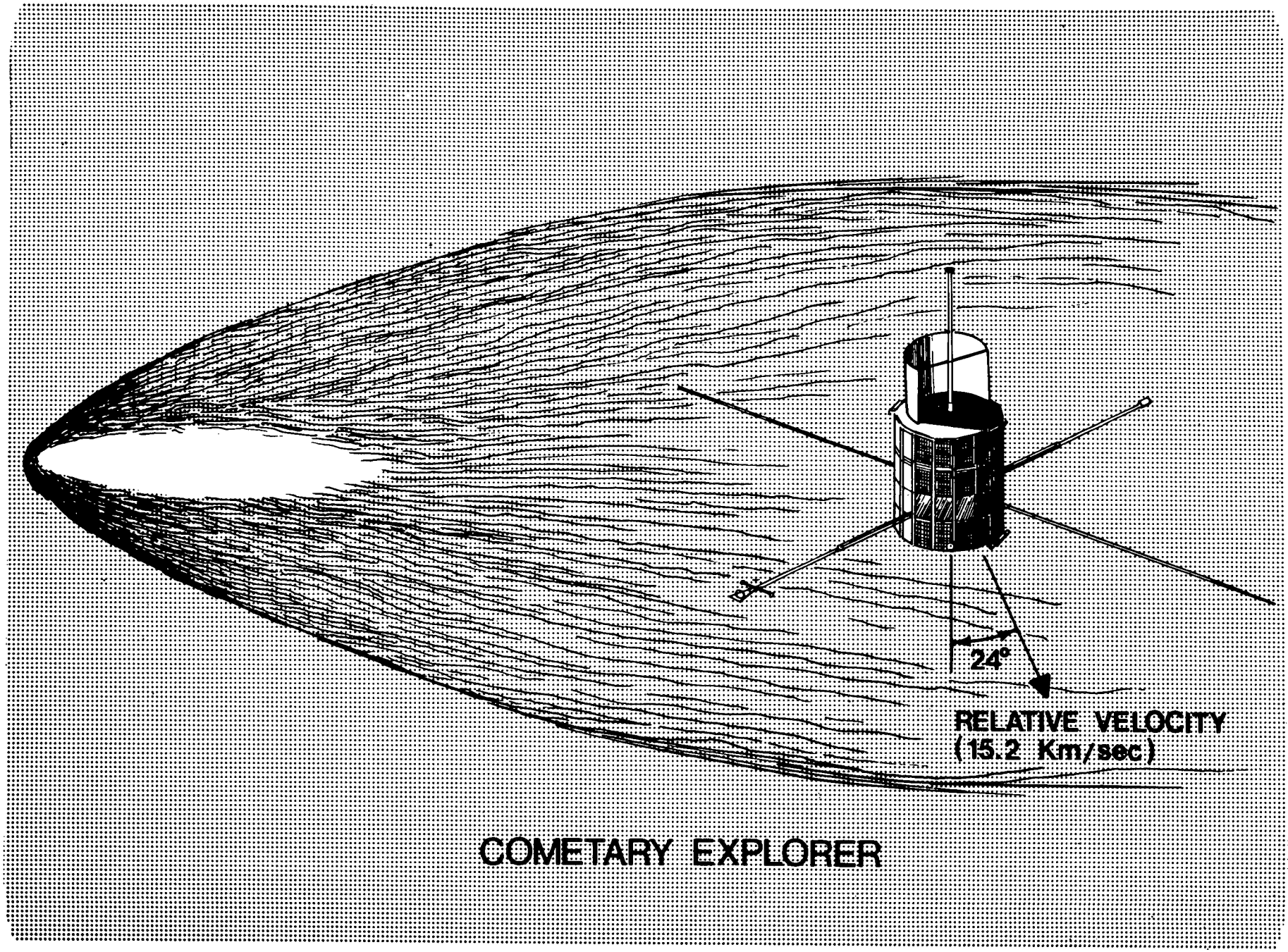

COMETARY EXPLORER

Frontispiece

TABLE OF CONTENTS

Cometary Explorer to Grigg-Skjellerup 1977

List of Figures

TABLES

Introduction

During the past decade, many notable developments in research related to cometary phenomena directly and indirectly have taken place. This includes advances in spectroscopy, photometry, orbital calculations, observations of ion tails, measurement of the solar ultraviolet spectrum and theoretical studies of the nucleus, coma, ion and dust tails, and experiments on cometary ions and molecules. Even more important is that a detailed in situ study of the supersonic solar wind flow has been accomplished by satellites and spacecraft. Dramatic observations of vast atmospheres of atomic hydrogen surrounding comets Tago-Sato-Kosaka (1969g) and Bennett (1969i) have also been performed from spacecraft and rockets.

We believe that it is now a most favorable opportunity to consider the implementation of a direct probe to a comet in the near future. By combining our experience gained in the conduct of space experiments during the past decade in studying the solar wind, its composition and its interaction with the earth and moon, with our spacecraft and mission development concept, management and analysis experience, we are in a very favorable position to present a specific cometary mission during the late 1970's. This initial cometary mission will provide much useful information concerning the atmosphere of the comet and its composition and interaction with the solar wind, thus providing a firm basis for more ambitious cometary missions in the 1980's.

The Cometary Explorer to Grigg-Skjellerup in 1977 is a mission which has been developed taking into account scientific, technical and management considerations. It is a mission whose scheduling and costs are very realistic, considered from several view points, since essentially zero technological development is required. This is because the mission utilizes as a "laboratory bench" for the instruments a spacecraft system already developed in the earlier IMP programs. The only costs to be incurred are required for fabrication of S/C subsystems rather than in development costs of new subsystems. In addition, the use of an existing spacecraft program in which the scientific mission objectives have been related to the studies of the solar wind, and interactions with planetary objects, implies that the basic spacecraft concepts already provide for support of those experiments particularly relevant to the scientific objectives of a cometary mission.

The purpose of this first mission to a comet would be as a precursor to larger missions both in scope and costs. This first mission would concentrate on a study of the nature of the solar wind interaction with a cometary coma, answering specific questions such as: does a bow shock exist? If so, what is its scale size? what is the chemical composition of the coma? what are the energetics of the ions and electrons in the cometary atmosphere? what is the nature of the tail structure?

This study represents the efforts of a small group of scientists, spacecraft engineers and mission analysts interested in the possibility of a low cost feasible precursor mission. This study summarizes briefly the scientific background and objectives of such a mission and proposes typical experimental studies and appropriate instrumentation.

The main body of the report discusses the actual spacecraft system to be employed, especially the mission unique characteristics distinguishing it from the earlier IMP missions. The heritage of the highly successful IMP series includes the Explorer 35 or AIMP-E spacecraft, which has operated successfully in lunar orbit for more than 5 years, providing valuable data on the lunar environment. The other seven IMP spacecraft were in earth orbit, studying the details of our terrestrial magnetospheric environment and the interplanetary medium.

The basic spacecraft system, the same as Explorers 43 and 47, is sufficiently well developed that only a single spacecraft is carried throughout the launch schedule. However, for the scientific experiments, both a prototype and flight instrument are required. The proposed schedule takes into account the realities of project review and approval and presents the opportunity for an optimized mission through the use of a Science Working Team concept. The final experiment selection is contingent upon final spacecraft design and total costs evaluations. The Science Working Team will include not only experimenters interested in studies utilizing onboard instrumentation but also those investigators utilizing ground based facilities to observe various cometary phenomena. The closely coordinated effort between both ground based and space observations is essential in interpreting these in situ observational measurements and extrapolating them to other comets.

A particular comet was selected after much consideration of technical, scientific and fiscal constraints. The flyby velocity at intercept is only 15.2 km/sec, which should permit utilization of existing spacecraft instrumentation studying the chemical composition of the atmospheres of the earth and planets. Instrumentation to study the solar wind and its interactions is already well developed and no special problems are expected for the experiment repertoire (8 or more instruments).

A total of 150 lbs is available for experiment weight and 55 watts of regulated power (28V $\pm$2%). Telemetry bit rates at intercept are at least 3000 bps. These will support 8-12 experiments. Intercept times are on the order of 5 hours, depending upon the cross section assumed for the interaction region between the cometary atmosphere and the solar wind. A realizable schedule is included in this report and cost estimates have been obtained and can be made available. For reference, the total run out costs of the 9 IMP's launched thus far is less than $\$75 \times 10^6$.

It should be noted that this proposed mission satisfies all of the recommendations of the Cometary Science Working Group (1971) and the Comet and Asteroid Mission Study Panel (1972) for a first mission to a comet (a fast fly-by to a short period comet in the late 1970's with investigation of the cometary atmosphere and coma/nucleus using an existing chemical propulsion system).

1.0 Origin and Nucleus of Comets

Comets, once thought to be portents of future events, are now recognized as scientific indicators of present conditions in interplanetary space and past conditions in the primordial solar nebula. Through December 1971, a total of about 610 comets have been observed. These are nearly all observations of the cloud of gas and dust emitted from the nucleus, not the nucleus itself. According to the generally accepted ideas of comets, the nucleus is an icy conglomerate of frozen gases and meteoritic material about 1-50 kms in diameter. As it approaches the sun, solar energy causes the release of material from the nucleus. Neutral molecules produce a more or less circular coma. Ions and dust, if in sufficient quantity, give rise to two types of elongated tails. The ion tail points nearly radially away from the sun whereas the dust tail is somewhat curved and tends to lag along the trajectory behind the comet (see Figure 1.1).

The classification of 610 comets in Table 1 is according to orbital periods. "Parabolic" comets are those with such elongated, long period orbits that the small observable arc cannot distinguish an ellipse from a parabola. No comet orbits are believed to have been initially hyperbolic far beyond the distance at which the orbits are perturbed by the planets. This would mean that all known comets are permanent members of the solar system. The column headed Abs. Mag shows the intrinsic luminosity of the comet measured by the luminosity in magnitudes it would have at 1 AU, from both the sun and earth. Table 1.1 emphasizes the intrinsic faintness of the comets with shortest periods.

TABLE 1.1

Statistics of Comets

Period	No.	Inclination	Abs. Mag.	Diam. (km)
Periodic, < 200 years	101	$< 30^{\circ}$	> 10	0.2 - 10
Periodic, > 200 years	133	nearly random	2 - 12	1 - 50
"Parabolic"	376	Random	3 - 10	1 - 50

Estimated total in Solar System Comet Cloud: 10^{8} - 10^{11}

The composition of the nucleus is a mixture of all the species observed in the spectra, presumably in a more stable form than the observed radicals. Table 2.1 lists the observed species and possible parent molecules of the observed radicals. A satisfactory working model for the nucleus consists of a "dirty snowball". This is largely ordinary ice containing various proportions of the other species listed. During each perihelion passage about 0.1% of the nuclear mass is lost. An important consequence of mass loss by vaporization is the cooling of the nucleus. An ice nucleus remains below about 250°K to within a few tenths of an AU.

These aggregates are generally believed to have accumulated from the outer regions of the primordial solar nebula at the same time as did the planets. Several investigators, e.g., Whipple, Opik and Kuiper, have proposed that the giant outer planets are accumulations of comet-like objects with additional hydrogen and helium that could be retained when the gravitational attraction of these planets becomes large enough.

The presently observed comets are objects which escaped capture by these planets. In order to have survived gradual disintegration during the five billion years since the epoch of formation they had to have been in orbits which never took them within about 50 AU of the sun. Oort has proposed an enormous Comet cloud at about 10^5 AU containing some 10^{11} objects. There are several difficulties with the details of this hypothesis but in some form it probably contains the essential features of the formation and preservation of comets. The accumulation of the comets may have been associated with the collapse of a large cloud forming a star cluster rather than with an isolated solar nebula.

Regardless of the details, the preservation of the nucleus means that it was subjected to minimum external heating effects. Because of their small size and mass, gravitational compression was also negligible. Radioactive decay may have produced some heating effects in the central core. However, it seems unlikely that any major structural or compositional changes have taken place throughout most of the cometary nucleus during the long period when it was far from the sun. Comets thus represent relatively unchanged aggregates that formed in a collapsed interstellar cloud about the same time as the planets. It is also likely that cometary objects were the precursors of the giant planets. Thus, an investigation of cometary properties is essential to understanding the formation of the non-terrestrial planets.

STRUCTURE OF COMET

1. COMA ONLY — GRIGG - SKJELLERUP

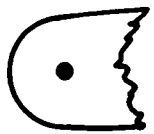

2. COMA - TRACE OF ION TAIL — ENCKE

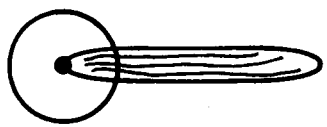

3. COMA - PROMINENT ION TAIL — HALLEY
~25% OF ALL COMETS

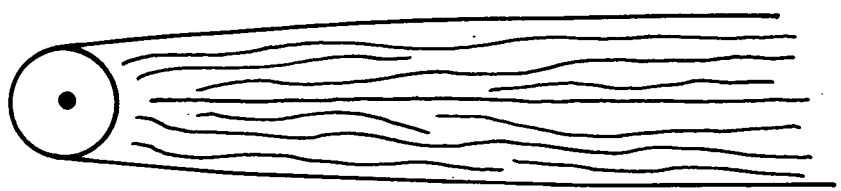

FIGURE 1.1

2.0 Mission Scientific Objectives

2.1 Phenomena in the Coma and Nucleus

This section addresses itself to the principle features of the atmospheres of comets, the major scientific questions concerning this atmosphere, and the type of experiments that could be done to answer some of these questions. The principle features of comets are summarized in Figure 2.1. Throughout this discussion the validity of the icy conglomerate model will be assumed. Recent OAO-2 results and studies by Marsden on the non-gravitational effects in comets strongly support this assumption.

Our current knowledge suggests that at large distances from the sun, (> 5 AU), the nucleus of a comet is in radiative equilibrium with the solar radiation. As the comet approaches closer to the sun, the ice starts to sublimate releasing micron size dust particles and molecules, such as H_2O, HCN, etc., which are the precursors of the observed radicals. The short wavelength light from the sun then dissociates these molecules into radicals and atoms. These fragments represent the emitters that are observed in the coma of the comet. At the present time we do not have an adequate explanation of the magnitude of the ionization nor the motion of the ions observed in comets.

A summary of the identified molecular, ionic and atomic emissions observed in comets is given in Table 2.1 along with suggested parents of these unstable species. These suggested parents are taken from the list of observed interstellar molecules. Of this list, only H_2O is reasonably certain and even it has not been identified directly. Thus a major scientific question in cometary astrochemistry is the identity of the parent compounds. An answer to this question would be invaluable in increasing our knowledge of the early history of the solar system. Furthermore, knowing the identity of the precursors of the unstable species in comets is a necessary condition in understanding how these unstable species are formed in a cometary atmosphere.

Table 2.1

Observed Radicals	Possible Parent
H	H_2O etc
O^1D	H_2O
OH	H_2O, CH_3OH
CN	C_2N_2, CH_3CN, HCN, HC_2-CN
CH	CH_4, CN_3CN, H_2C_2, CH_3C_2H
NH (Singlet)	NH_3, HNCO, NH_2HCO
NH_2 α bands	NH_3, NH_2HCO
C_2 Singlet and triplet	C_3, HC_2CN, CH_2C_2H, C_2H_2
C_3	$H_2C = C = CH_2$, $CH_3 - C = CH$, HC C - C $\equiv$CH
CO^+	CO
N_2^+	N_2
Ni, Cu, Ca, Cr, Fe, Mn	Observed in sun grazing comets at less than 0.1 astronomical units where grain temperatures are $\sim 1000^{\circ}K$

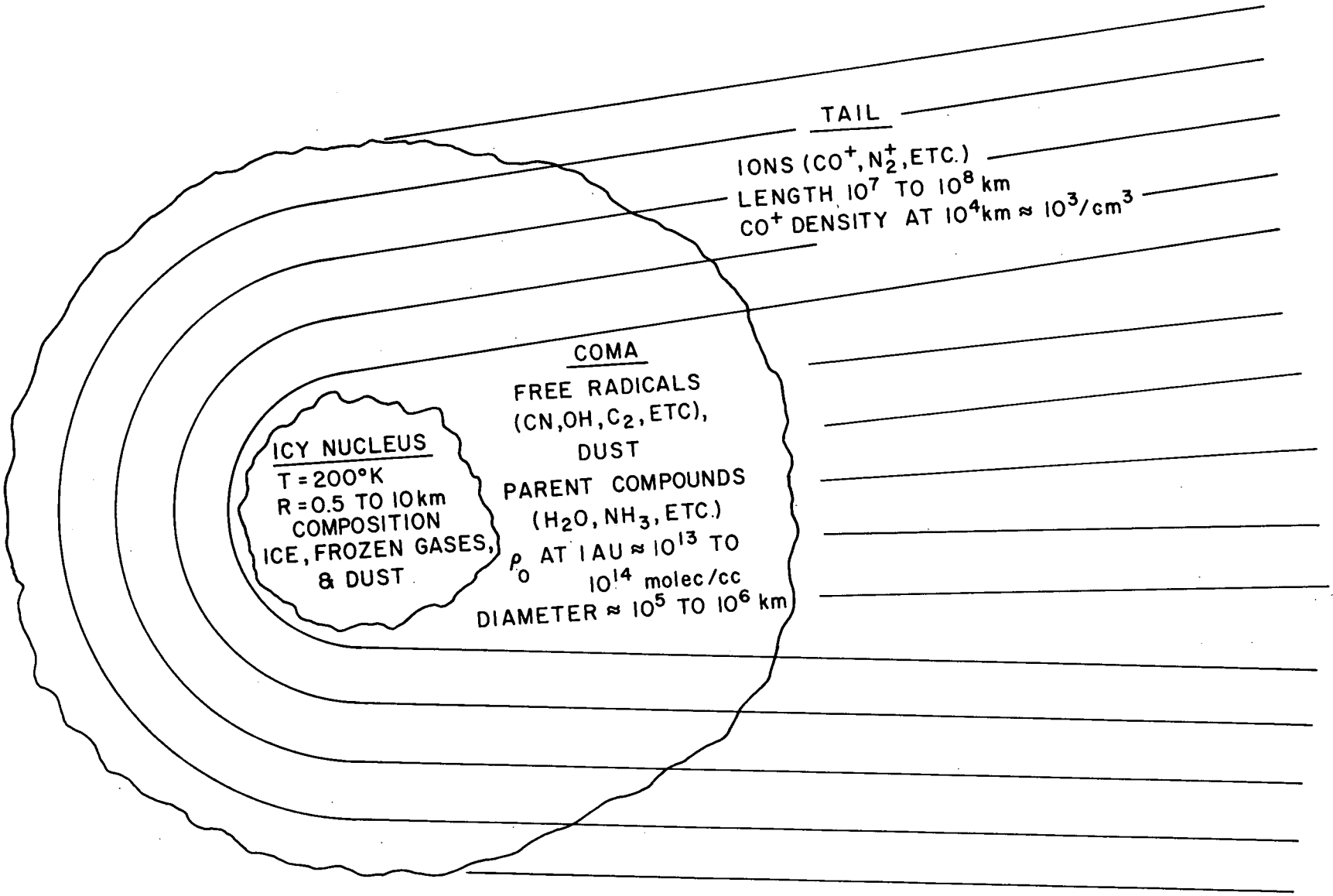
TAIL
IONS (CO^+, N_2^+, ETC.)
LENGTH 10^7 TO 10^8 km
CO^+ DENSITY AT 10^4km ≈ 10^3/cm^3
COMA
FREE RADICALS
(CN, OH, C_2, ETC),
DUST
PARENT COMPOUNDS
(H_2O, NH_3, ETC.)
ρ_0 AT 1 AU ≈ 10^{13} TO
10^{14} molec/cc
DIAMETER ≈ 10^5 TO 10^6 km
ICY NUCLEUS
T = 200°K
R = 0.5 TO 10km
COMPOSITION
ICE, FROZEN GASES,
& DUST

FIGURE 2.1

Another question of importance in comets is the size distribution and chemical composition of the dust. This information is helpful in determining what were the physical conditions during the formation of the comet. Such data about dust would contribute to a better understanding of the accretion processes that formed the planets.

Thus the first three basic scientific questions about the coma and nucleus of a comet are:

1. What is the identity of the parent molecules?
2. How are the ions and radicals formed?
3. What is the dust composition and size distribution?

Under "Identity of the parent molecules", the most general detector system to be used is a mass spectrometer since it would identify any molecules in the vapor phase. However, specific molecule detectors could also be designed, such as a vacuum ultraviolet lamp, or an electron beam that might dissociatively excite parent molecules such as H_2O, HCN, NH_3, etc. The excited molecular fragment could then be detected with a filtered photomultiplier.

Our understanding of the formation of radicals and ions in comets is also limited by our lack of firm knowledge about the conditions in the coma of comets. A straight through ion gauge and a closed off ion gauge would tell us what the total gas density and flow velocity of the gas is in the comet. This can be compared with the theoretical predictions of the icy congomerate model of the nucleus. Total ion composition should also be measured in the coma, not just those ions which have fluorescence spectra in regions that can be observed. An impact mass spectrometer and a cosmic dust detector will provide information on what the elemental composition of the dust is and the size, mass and velocity of the dust.

2.2 Solar Wind-Cometary Atmosphere Interaction

The structure, appearance, and behavior of the coma and ion tail of a comet are strongly related to its interaction with the solar wind. This interaction may also be an important factor in cometary decay. Because of the importance of the solar wind interaction, it is essential to choose a spacecraft trajectory and scientific payload which will determine the most important features of this interaction. The following paragraphs discuss the key problems, the measurements which are needed to solve these problems, and the general scientific significance of the results so obtained.

Short period comets such as Giacobini-Zinner have no observable ion tail or as in the case of Comet Encke only a trace of one although there must be some ions present. These either do not radiate in the visible region of the spectrum or have too low a concentration to be detectable

The four key questions related to the interaction phenomena are:

BOW SHOCK AND CONTACT SURFACE

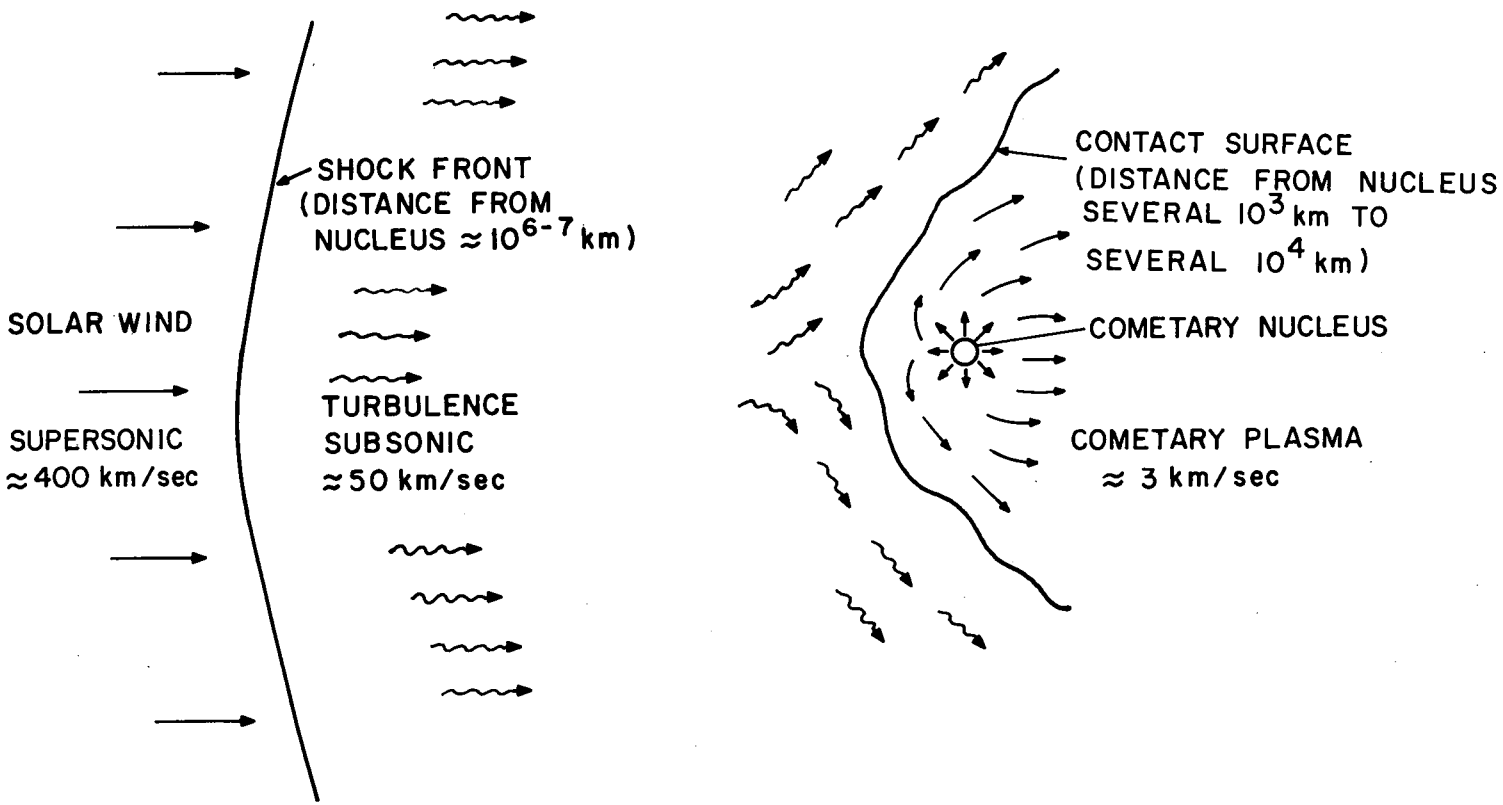

FIGURE 2.2

4. What is the qualitative nature of the interaction and how is the solar wind flow diverted around the coma?
5. What are the dominant ionization processes in the coma?
6. At what rate and by what mechanisms are the various types of particles removed?
7. What is the structure of the tail and how does one explain the various motions observed in the comet-ion tails?

2.2.1 Nature of the Interaction and Basic Flow Pattern.

The solar wind interacts with the gases and plasmas in the coma. Two radically different types of interactions have been proposed recently, neither of which can be excluded at moment. Biermann and his colleagues have developed models which postulate a bow shock and contact surface analogous to those of the earth and its magnetosphere. In particular, these models imply a discontinuous transition from supersonic to subsonic flow. Wallis (1971) on the other hand, has suggested that the transition from supersonic to subsonic flow is continuous, over a very broad region, occurring without a bow shock. These two models are diametrically opposite, indicating how little we actually know about the interaction.

Of the two models just mentioned, the bow shock-model has been developed in greater quantitative detail. It predicts a standoff distance for the shock of (1 to 2) x 10^6 km and a corresponding distance for the contact surface of (1 to 5) x 10^5 km. (Brosowski and Wegman, 1972). The latter is comparable to the typical size of a visible coma. The introduction of a contact surface is an idealization and its validity may be questioned. For example, by definition a contact surface implies no flux through the surface, but observations(Wurm, 1963) indicate the filaments of ionized material from near the nucleus probably penetrate the "contact surface" on the sunward side, and then bend back into the tail region.

The magnetic field probably plays a key role in the structure and behavior of comets, as suggested first by Alfven (1957). Given the flow pattern, it is possible to calculate the magnetic field configuration -- if the field is frozen-in to the plasma. However, it is possible that in the coma the field is not frozen-in to plasma. The transition between "frozen" and "unfrozen" conditions is of basic physical interest as well as being important for understanding cometary ion tail dynamics. The configuration of the magnetic field in the coma is strongly affected by (and may strongly affect) the flow pattern. For example, if the flow past the coma is analogous to the flow past the magnetosphere, as Biermann suggests, then the field is draped around the coma on the sunward side. Unlike the earth's magnetosphere, however, the coma probably has no

magnetic field of its own, so the configuration should be unstable with respect to the Rayleigh-Taylor instability, i.e. a stable contact surface will not persist. In this case, the solar wind might penetrate more deeply into the coma than Biermann's models suggests, and conversely the instability might explain how matter can flow outward from the nucleus.

Clearly, to determine the dynamics of the interaction, the basic measurements that are needed are of velocities, densities and temperatures of ions and electrons and the magnetic and electric fields, ideally on the sunward side of the comet, from a few times 10^6 km to at least 10^4 km from the nucleus.

2.2.2 Ionization Processes.

An understanding of the ionization processes in comets is essential for understanding the chemistry of comets and the solar wind-comet interaction. To fully understand the ionization processes, it will be necessary to determine which ions are present and from which neutrals they are derived. An ion mass spectrometer with a mass per charge range from 1 to approximately 80 and a speed range between 0 and 300 km/sec and a neutral mass spectrometer are needed for this purpose. Ideally, one would like to survey the distribution of these materials in the coma tail, and the region outside the visible coma.

Given the ions, one may then ask how they are produced. Photoionization is undoubtedly important in comets. Another ionizing mechanism is charge exchange between the solar wind and cometary atmosphere material. Recent measurements indicate that this is more important than photoionization, the rate of charge transfer reactions being 3 times that for photoionization (Biermann and Lust, 1972). Photoionization and charge exchange alone, however, cannot explain all of the observations of ions (Delsemme, 1971), so other processes must be considered.

Energetic (kev) electrons are a particularly effective and a likely ionizing agent (Delsemme, 1971). Thus, it is essential to at least survey the population of energetic electrons in the range 3 eV to 50 kev in and near the coma. Just how they are accelerated is not known. They might be accelerated in the bow shock (if it exists) or by particle-wave interactions in the coma, as they are near the earth. To determine whether particle-wave interactions are important, a survey of high frequency electric and magnetic field fluctuations would be essential on an early comet mission.

Laboratory experiments (Danielsson, 1972) show that when a collisionless magnetized plasma interacts with a neutral gas, the gas becomes ionized. The ionization process is not understood, but it is clearly a plasma mechanism rather than a classical

ionization process. It will be important to determine to what extent such plasma or collective ion-field processes occur in comets and, ultimately, to understand these processes.

2.2.3 Mass Loss.

The lifetime of a comet depends on the rate at which it looses mass while the composition depends upon how it looses mass. Several mechanisms of mass loss may be important. Neutrals may simply evaporate, oblivious to the existence of the solar wind and magnetic fields. Ions and electrons will be swept away by the flow of magnetized solar plasma. Some ions will be produced from neutrals in the coma and in regions farther away. These will immediately begin to orbit any magnetic field lines that may be presented and will move with the field lines. Thus, they too may be carried away from the comet by the magnetized flow. Clearly, then, the cometary atmosphere is steadily eroded by the solar wind. Not all materials will be removed at the same rate or in the same way, so the erosion process will cause a fractionation of the comet's constituents. Of particularly interest is the manner in which material is carried into the tail of the comet.

2.2.4 Structure and Motions of Comet Tails.

This subject has been of popular and scientific interest for centuries. It has challenged Newton himself, and Bessel too, but neither could explain the observations. Their failure is probably the result of considering only mechanical interactions and not realizing the importance of electrodynamic processes in comets.

Not all comets have visible tails. However, visible tails are due to the ions CO^+ and N_2^+ CH^+ etc. (Richter, 1963), are clearly minor constituents. One expects some flow of material into the tail region for all comets, for the reasons discussed in the previous section. For comets with visible tails we know that this flow extends to a distance up to 1 AU. The corresponding extent of flows in comets without visible tails is unknown.

Of first importance is the determination of the structure of the tail: its dimensions, composition, average flow pattern, and the magnetic field configurations. A single fly-by through the tail at $\approx 10^6$ km would provide such basic information. With sufficiently high sampling rates one could also resolve the fine structure and determine, for example, the nature of the rays and filaments which are usually observed. A variety of non-steady motions has been observed. These motions include waves, kinks, helical perturbations, and "turbulent" motions.

Such motions do not always occur, and will probably not be seen on a single flyby. They could best be studied with a rendezvous mission. However, if the basic structure of the tail were determined on a fly-by, one could probably immediately exclude a number of theories of such motions and it might even be possible to arrive at some positive conclusions about the nature of such motions.

More important than the type of motions just described, are the steady accelerations observed both along and transverse to the tail. A single fly-by cannot unambiguously separate these two velocity gradients, but the gradient along the trajectory will be determined. Combining this with a model of the basic solar wind-comet interaction might give fairly complete knowledge of the velocity field. Obviously, the instruments needed for a study of the tail are essentially the same as those described earlier-magnetometer, electric field detectors, plasma analyzers and mass spectrometers.

3.0 Mission Analysis

3.1 Comet Recovery and Earth-Based Observations

The orbital parameters for the 1977 apparition of Grigg-Skjellerup are given in Figure 3.1. In computing the 1977 orbit, nongravitational coefficients from 1942-1962 were assumed (Marsden, 1972), and the initial conditions were obtained from the 1956-1966 observations. The same inputs were used to predict the 1972 perihelion date that was within 0.01 days of the observed time. Therefore, the present orbit is very well known, and its accuracy should be further improved when the 1972 observations are included in the 1977 ephermeris calculation.

The indicated a priori orbital accuracy for Grigg-Skjellerup justifies a pre-recovery launch. Before recovery, the uncertainty of the comet's orbit would result in a miss-distance between the spacecraft and the comet of about 30,000 km. However, after recovery, new observations should reduce this error to less than 1000 km. The propulsive maneuvers that would be needed to correct the spacecraft's trajectory to account for the updated comet orbit would be quite small.

As can be seen in Figure 3.1, the favorable orbital geometry in 1977 is conducive to an early recovery. If it is postulated that recovery will occur when the comet attains a nuclear magnitude of 18, the recovery date would be about December 1, 1972, which is more than four months before intercept. This estimate is somewhat more conservative than that given in previous studies (JPL and Friedlander et al., 1971) where recovery is assumed to occur at 20th magnitude.

Because one to two hours are needed for proper exposure of the recovery photograph, proper sighting conditions at the earth observatory are also required. At the estimated recovery date, there will be about five "dark" observing hours per day at a 35°S latitude site and approximately six hours at a 35°N latitude site, which is more than adequate. The comet is considered to be observable when it is located 25° above the local horizon in a dark sky (sun 18° below the horizon). Earth-based sighting conditions before and after the planned encounter date (April 11, 1977) are given in Figure 3.2. Notice that there will be a rather long gap in comet observability from a 35°N latitude site before encounter. Therefore it will be necessary to rely on sightings from observatories located in the southern hemisphere during this period.

The variation in the comet's brightness is plotted in Figure 3.3. Nuclear magnitude refers to the stellar brightness of the comet's central condensation and is used primarily for recovery and orbit determination. Total magnitude is a measure of the comet's total brightness (including coma and tail emissions) and is useful for evaluating conditions for earth-based spectroscopic measurements. A total magnitude of 12 is an approximate limit for the spectroscopic measurements.

EPOCH	APR. 7.0, 1977
TIME OF PERIHELION	APR. 11.017, 1977
PERIHELION DISTANCE	0.993 AU
APHELION DISTANCE	4.932 AU
ECCENTRICITY	0.665
INCLINATION	21.10°
PERIOD	5.10 YEARS
LONGITUDE OF NODE	212.64°
ARGUMENT OF PERIHELION	359.32°

ORBIT PROJECTION IN ECLIPTIC PLANE

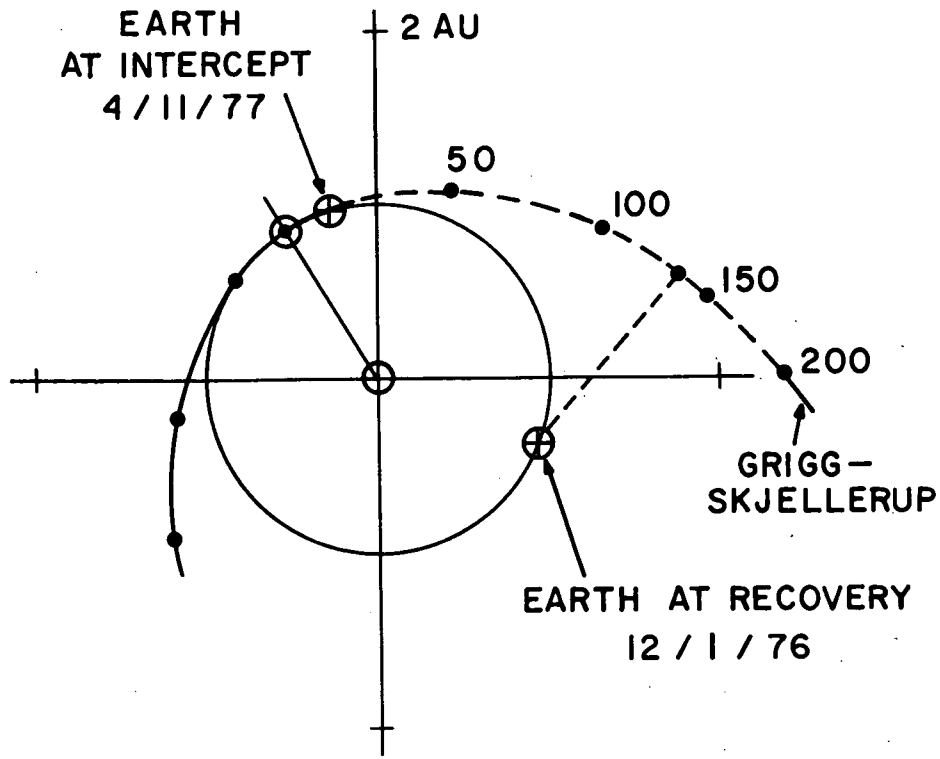

——— ABOVE ECLIPTIC

– – – – – BELOW ECLIPTIC

• COMET AT STATED NUMBER OF DAYS BEFORE OR AFTER PERIHELION

⊙ COMET AT PERIHELION AND ECLIPTIC INTERSECTION

FIGURE 3.1

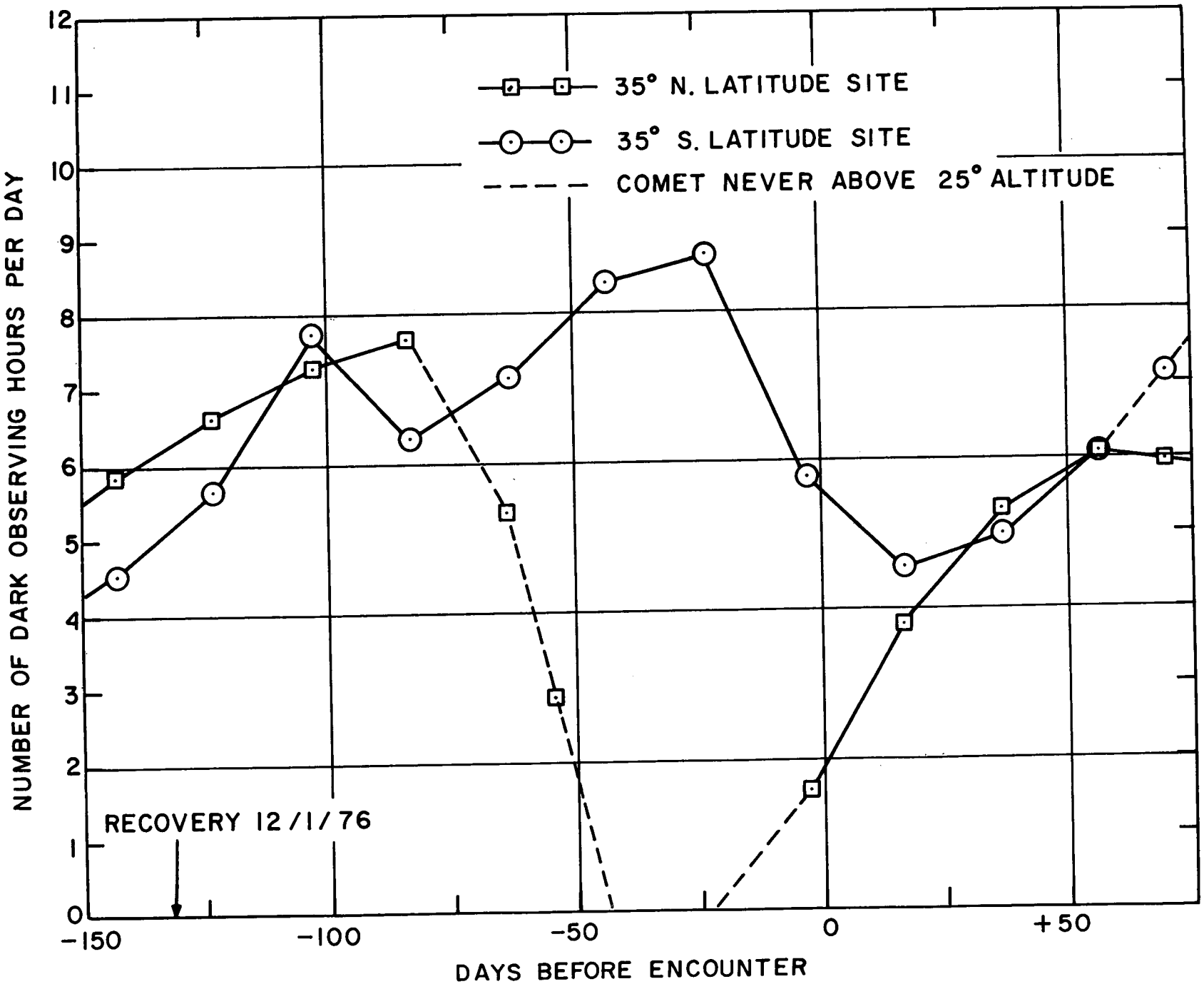
35° N. LATITUDE SITE
35° S. LATITUDE SITE
COMET NEVER ABOVE 25° ALTITUDE
NUMBER OF DARK OBSERVING HOURS PER DAY
RECOVERY 12/1/76
DAYS BEFORE ENCOUNTER
0
1
2
3
4
5
6
7
8
9
10
11
12
-150
-100
-50
0
+50

FIGURE 3.2

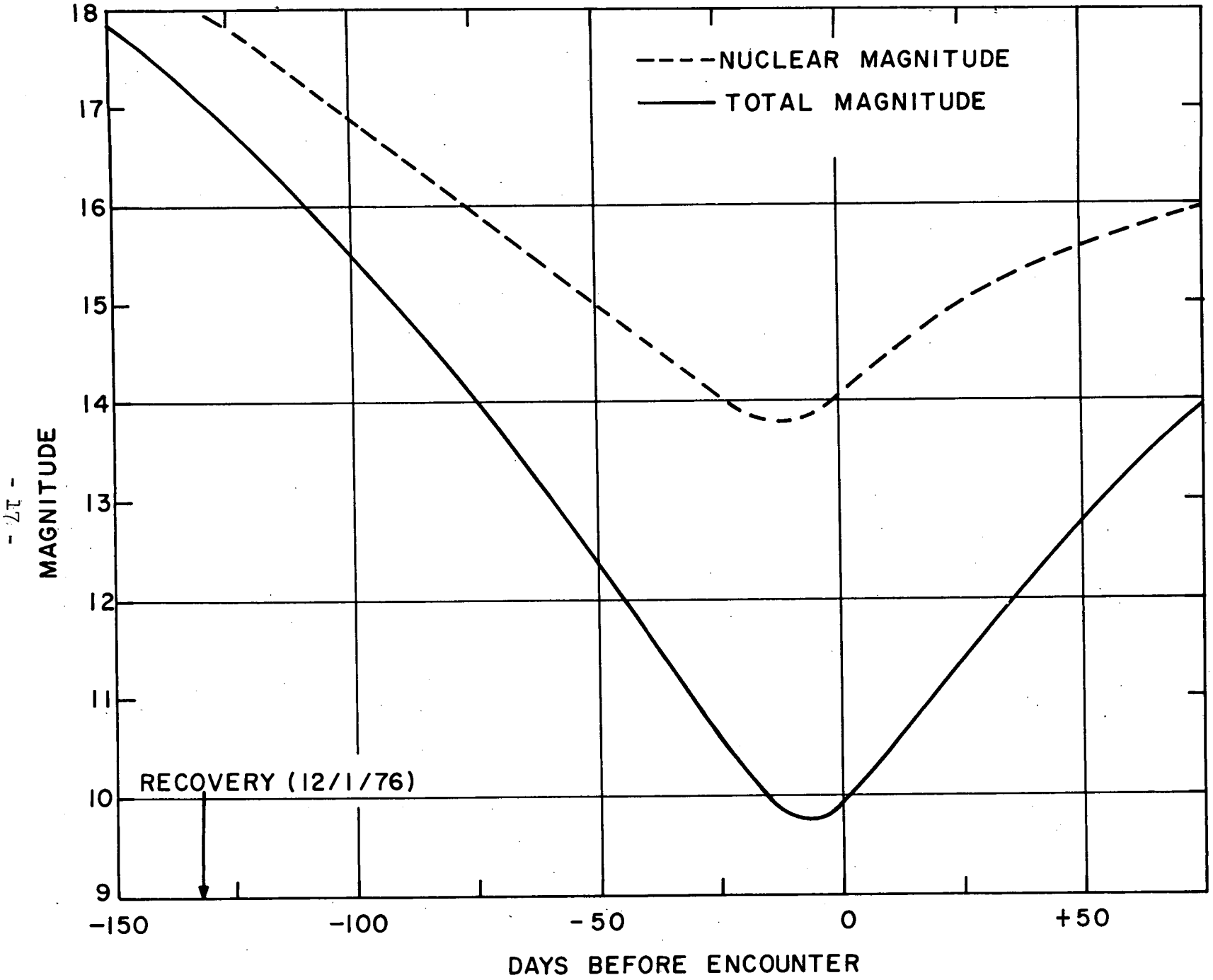
----NUCLEAR MAGNITUDE
—— TOTAL MAGNITUDE
RECOVERY (12/1/76)
MAGNITUDE
DAYS BEFORE ENCOUNTER
18
17
16
15
14
13
12
11
10
9
-150
-100
-50
0
+50

FIGURE 3.3

3.2 Mission Description

The nominal mission profile is summarized in Figure 3.4. To minimize the launch energy requirement (C_3), it was decided to intercept Grigg-Skjellerup as it crossed the ecliptic plane which occurs about a 1/2-day after the comet's perihelion passage. This specification yielded a nominal C_3 value of only 2.37 km^2/sec^2. The comparatively inexpensive Delta-2914 launch vehicle should have no difficulty meeting this C_3 requirement. Assuming a spacecraft weight of 950 lb (432 kg) and adding 22 lb. for the #1809 attach fitting, the total useful load would be 972 lb. From Figure 3.5 it can be seen that the Delta-2914 can accommodate this load when $C_3 < 3.2$ km^2/sec^2.

Flight time from launch to the comet intercept is 158.5 days. Conditions at the cometary encounter are almost ideal. The relative velocity vector is only 15.2 km/sec, and the angle between the relative velocity vector and the spacecraft's spin axis is 24.6°. This angle, which is termed the relative aspect, is an important parameter for considering those experiments measuring the composition of the cometary coma. The small value of the relative aspect is rather fortuitous because antenna-pointing constraints require the spacecraft's spin axis to be perpendicular to the ecliptic plane. Another feature of the cometary encounter is that the comet will be close to its maximum brightness, having a total magnitude of 10.

In Figure 3.4A it can be seen that the spacecraft is placed into a trajectory that not only intercepts the comet, but also returns to the earth. The purpose of this extended-mission strategy is to carry out more scientific investigations of previously unexplored regions of the earth's magnetosphere, especially in the geomagnetic tail between 80 and 500 earth radii. Due to the high degree of commonality of the scientific instrumentation for many of the cometary and magnetosphere experiments, the earth-return extended mission mode is very attractive.

When the spacecraft returns to earth, the TE-M-458 solid retromotor is used to brake it into a high-apogee earth orbit. As shown in Figure 3.4B, the spacecraft eventually enters the geomagneic tail and spends about four months in the area near the sun-earth L_2 libration point. According to the Gylden-Moulton hypothesis, the gegenschein may be caused by dust particles temporarily trapped in this region. In-situ analysis using the cometary solid particle detectors could settle this issue. It should be pointed out that the geocentric trajectory is extremely sensitive to retro-firing errors and lunar perturbations, and its final form may be quite different than that shown in Figure 3.4B. However, the trajectory can easily be shaped to the desired form by applying small thrust corrections (using the hydrazine system) at the proper times.

3.3 Launch Window and Maneuver Budget

Although there is only one trajectory that returns to the vicinity of the earth when the comet intercept date is fixed and transfers that are longer than one year are not allowed, it is possible to open the

LAUNCH NOV. 4, 1976

C_3 = 2.37 Km^2/sec^2

COMET INTERCEPT APRIL 11, 1977

EARTH DISTANCE = 0.20 AU

RELATIVE VELOCITY = 15.2 Km/sec

RELATIVE ASPECT = 24.6°

EARTH RETURN OCT. 26, 1977

RETRO ΔV = 206 mps

PERIGEE = 14,000 Km

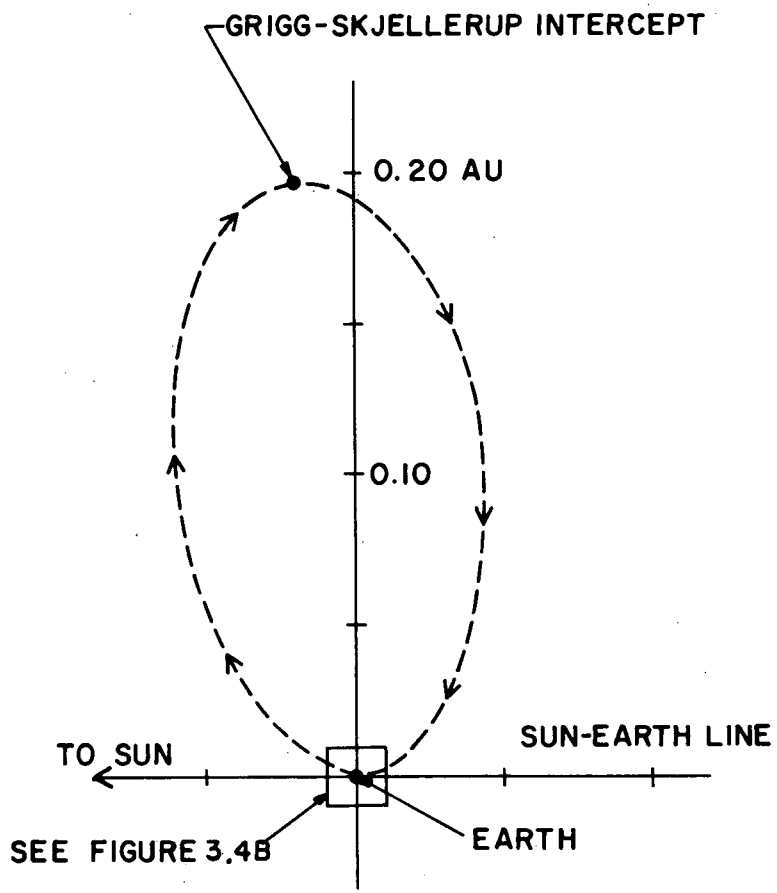

FIGURE 3.4A

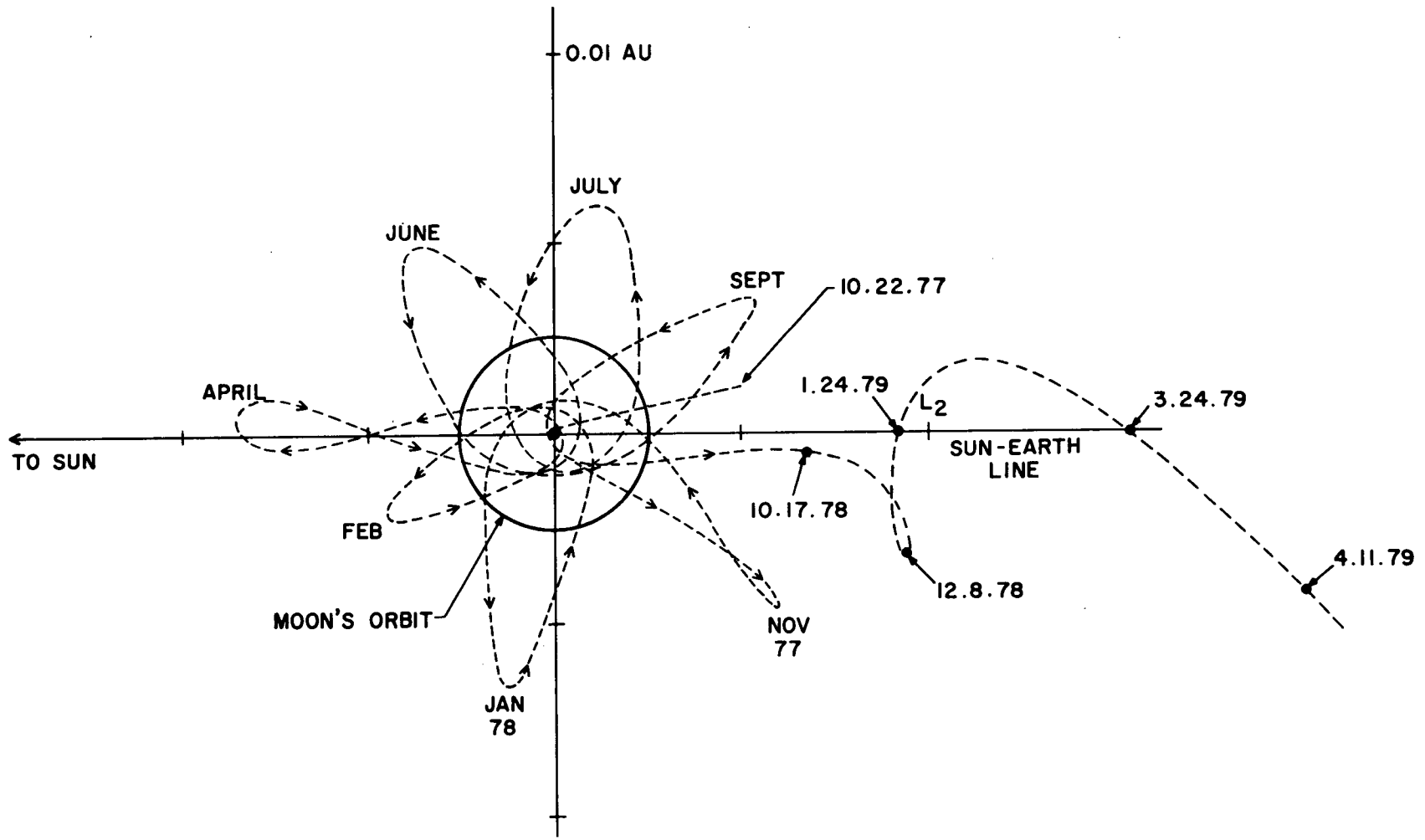
0.01 AU
JULY
JUNE
SEPT
10.22.77
APRIL
1.24.79
L2
3.24.79
TO SUN
SUN-EARTH
LINE
FEB
10.17.78
4.11.79
12.8.78
MOON'S ORBIT
NOV
77
JAN
78

FIGURE 3.4B

launch window by adding a modest velocity correction after the cometary encounter. The correction was specified to take place approximately 17.5 days after the encounter and the earth-return date was varied to minimize the required ΔV^*. The results of this investigation are listed in Table 3.1. Notice that $\Delta V_{AC} < 150$ mps for a two-week launch window. The launch energy requirement is also quite satisfactory during this period. Further optimization of the spacecraft weight and the hydrazine fuel budget should easily extend the launch window to three weeks.

Another mission parameter of interest in Table 3.1 is the declination of the launch asymptote (DLA). For range-safety reasons, unmanned interplanetary missions are currently restricted to using a southeast launch-azimuth corridor from Cape Kennedy with launch azimuths of between 90 and 114 degrees. Because of these launch-azimuth restrictions, interplanetary missions employing a parking orbit with optimum injection into the departure hyperbola require that the DLA be within $\pm 33^\circ$. There are also tracking and orbit-determination constraints that require the DLA to be $\geq 5^\circ$ in magnitude. In Table 3.1, it can be seen that these constraints are well satisfied during the entire launch window.

The earth-retro maneuver ΔV requirements listed in Table 3.1 have been determined by assuming a burn at a radius of closest approach (perigee) of about 14,000 km. Because the fuel loading of the TE-M-458 retro-motor has been fixed at 65 lb., the final radius for the burn will be a function of the actual earth-return date and the weight of the spacecraft at this time. The fuel loading has been sized by assuming an earth-return spacecraft weight of 900 lb. for the nominal mission profile.

The fuel loading for the hydrazine systems has been set at 200 lb. This loading should be adequate for all required velocity corrections as well as spin/attitude maneuvers. The hydrazine-system maneuver budget is listed in Table 3.2. Trajectory corrections before the cometary encounter would compensate for launch dispersion ($\sim$ 120 mps) and comet ephermeris errors ($\sim$30 mps). Note that there is a substantial amount of fuel remaining for orbital maneuvers after the spacecraft has returned to earth orbit.

*It is recognized that this procedure does not give the absolute minimum ΔV, but it is close to being optimal. A rigorous optimization of all trajectory corrections will be performed in the next phase of the mission study.

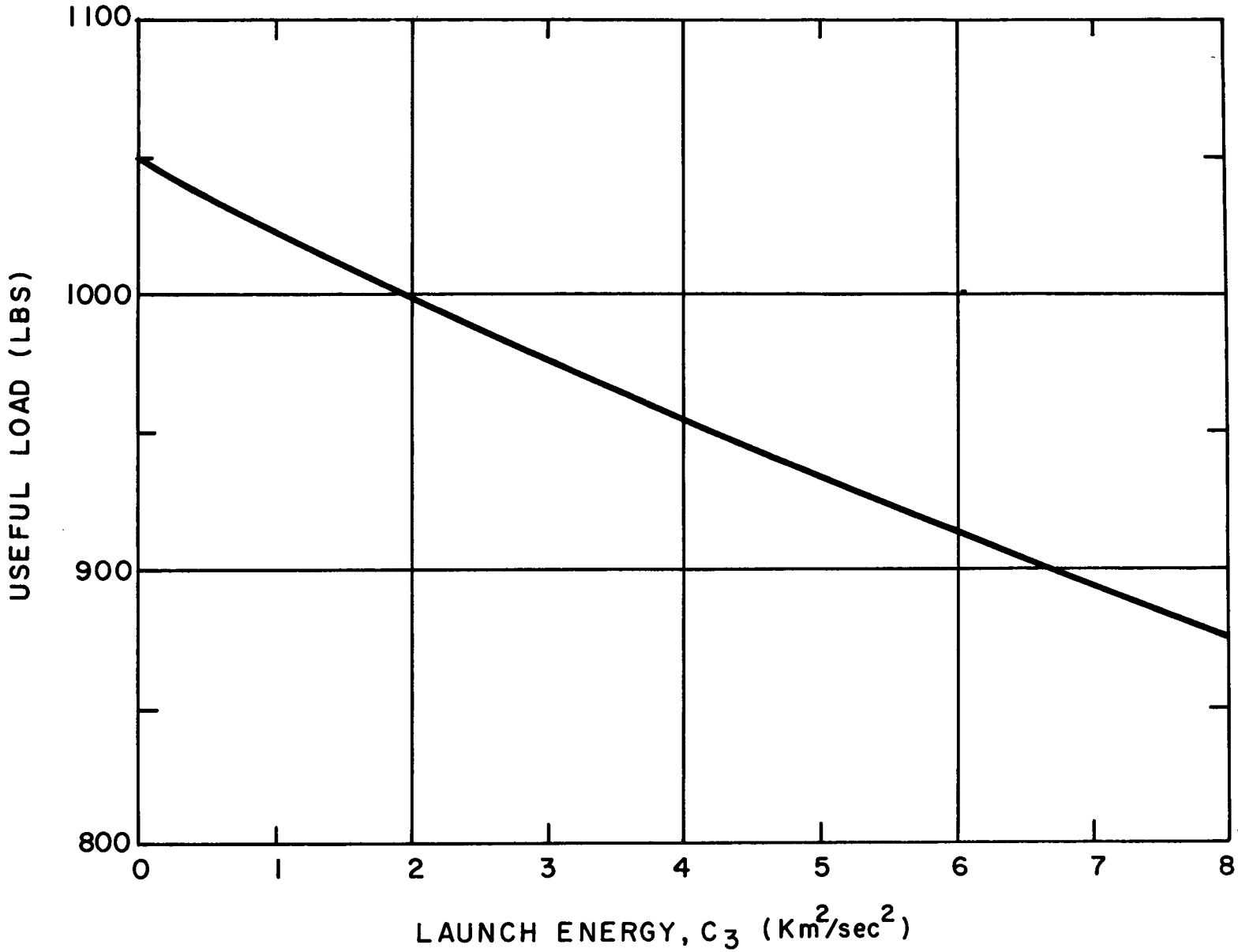
1100
1000
900
800
USEFUL LOAD (LBS)
0
1
2
3
4
5
6
7
8
LAUNCH ENERGY, C_3 (Km^2/sec^2)

FIGURE 3.5

TABLE 3.1

Launch Date	October 29, 1976	November 4, 1976	November 11, 1976
Launch Energy, C_3 (km^2/sec^2)	2.08	2.37	2.85
Declination of the Launch Asymptote	-14.35°	-15.68°	-17.14°
Inclination of Transfer Orbit (Heliocentric)	0.47°	0.12°	0.04°
At Comet:			
Relative Velocity (mps)	15.48	15.19	15.22
Relative Aspect	24.13°	24.55°	24.43°
Correction for Earth Return, ΔV_{AC} (mps)	146.93	11.44	135.65
Earth Retro Maneuver, $\Delta V_{\oplus}$ (mps)	209.66	205.64	226.23
Earth Return Date	October 28, 1977	October 26, 1977	October 19, 1977

MISSION PARAMETERS FOR TWO WEEK LAUNCH WINDOW

TABLE 3.2

	ΔV (mps)	Fuel Expenditure (lbs)
Trajectory Corrections (Comet Targeting)	150	65.22
Spin/Attitude Maneuvers	15	6.27
Trajectory Corrections (Earth Return)	175	69.95
Spin/Attitude Maneuvers	15	5.27
Geocentric Trajectory Corrections and Maneuvers	150	50.68
TOTAL	505	197.39

MANEUVER BUDGET FOR HYDRAZINE PROPULSION SYSTEM

4.0 Technical Summary

4.1 Spacecraft

The spacecraft is a continuation of the IMP-H, I and J series of spin stabilized spacecraft. The basic IMP-H, I and J design has been modified by extracting useful design concepts from Planetary Explorer, the German Solar Probe (HELIOS) and other appropriate spacecraft. The spacecraft is drum shaped, five feet long and approximately four feet in diameter. The spacecraft with the inclusion of the propulsion systems will weigh approximately 431 kilograms. Figures 4.1.1 to 4.1.4 present various views of the S/C.

The spacecraft will have the following subsystems essentially identical to IMP H and J

- o Thermal Control
- o Power System (increased solar cell cover glass for meteoroid protection)
- o Optical Aspect System

Subsystems Modified from IMP H, I and J (Explorers 43, 47 and ?)

- o Structure - modified to incorporate hydrazine, rocket motor, despun antenna
- o Harness - to accommodate new experiment repertoire

Subsystems Unique to the Mission

- o Mechanically Despun Antenna - Utilize HELIOS subsystem.
- o S-band Transmitter - Utilize Planetary Explorer subsystem
- o Hydrazine Subsystem - Utilize basic off-the-shelf components.
- o Solid Propellant Retromotor - Utilize AIMP-D and E (Explorer 33-35) Rocket Motor
- o Meteoroid Shielding (utilize Pioneer 10 design)
- o Command Subsystem - utilize design for follow-on IMP's
- o Data Handling - utilize design for follow-on IMPs
- o SCADS (Scanning Celestial Attitude Determination System) - utilize S3- A (Explorer 45) subsystem

4.2 RF Subsystem

Figure 4.2.1 shows the RF subsystem block diagram. The telemetry, command, and ranging functions will use a redundant S-band transponder system. The system will be made up of double-conversion superheterodyne command receivers, a transmitter for turnaround ranging and telemetry transmission, and diplexers with switches for directing the RF output to one of three antenna systems. The redundant command receivers will ensure command capability to the spacecraft regardless of its attitude or RF output mode. The communications system will be compatible with the facilities of the Deep Space Network (DSN) and use uplink and downlink frequencies of 2115 and 2295 MHz respectively. The transmitters will provide 1-, 5-, or 10-watt power output on command, with a corresponding power input of 6, 22, or 35 watts, respectively.

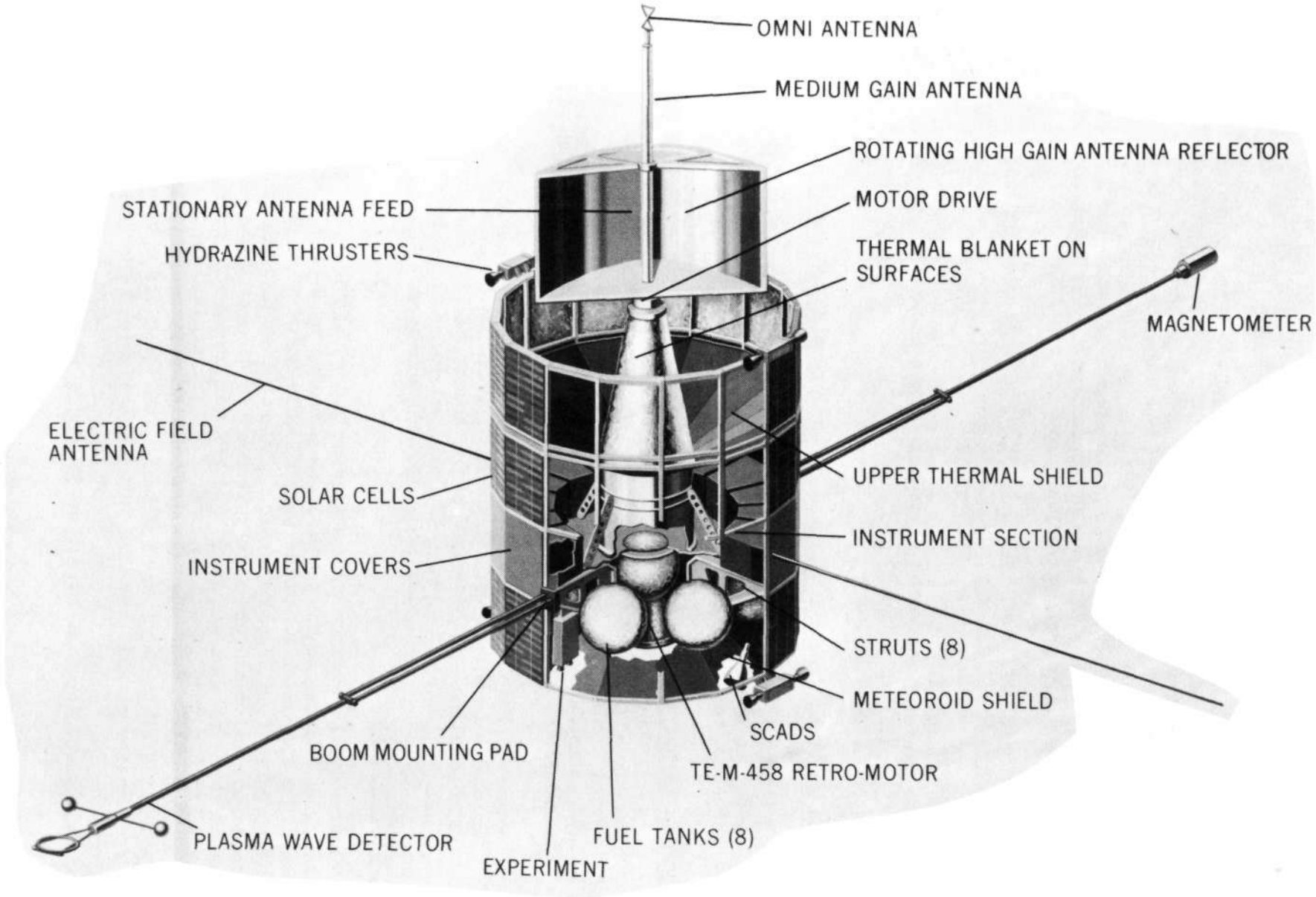
OMNI ANTENNA
MEDIUM GAIN ANTENNA
ROTATING HIGH GAIN ANTENNA REFLECTOR
STATIONARY ANTENNA FEED
MOTOR DRIVE
HYDRAZINE THRUSTERS
THERMAL BLANKET ON SURFACES
MAGNETOMETER
ELECTRIC FIELD ANTENNA
SOLAR CELLS
UPPER THERMAL SHIELD
INSTRUMENT SECTION
INSTRUMENT COVERS
STRUTS (8)
METEOROID SHIELD
SCADS
BOOM MOUNTING PAD
TE-M-458 RETRO-MOTOR
PLASMA WAVE DETECTOR
FUEL TANKS (8)
EXPERIMENT

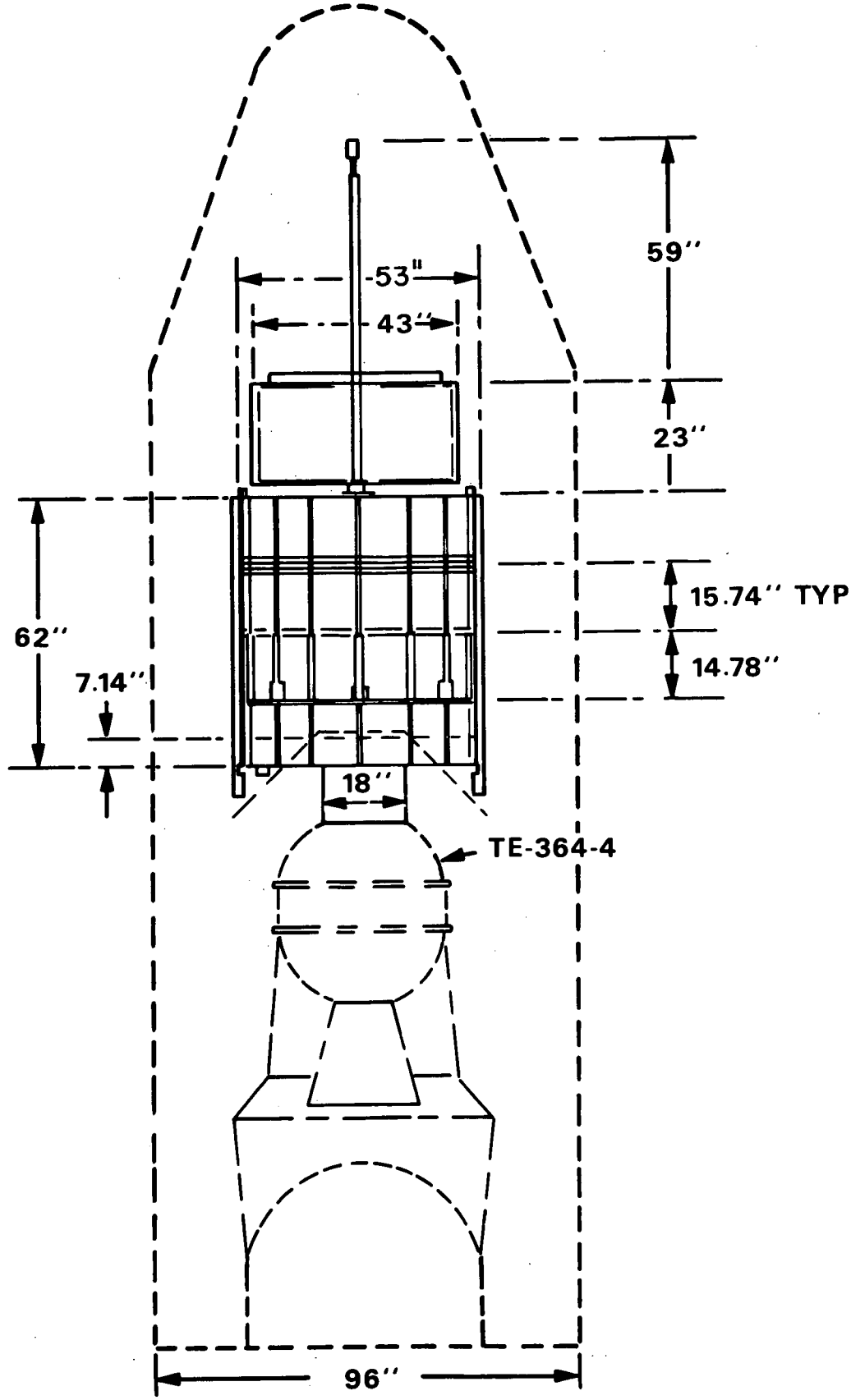

GENERAL LAYOUT

FIGURE 4.1.2

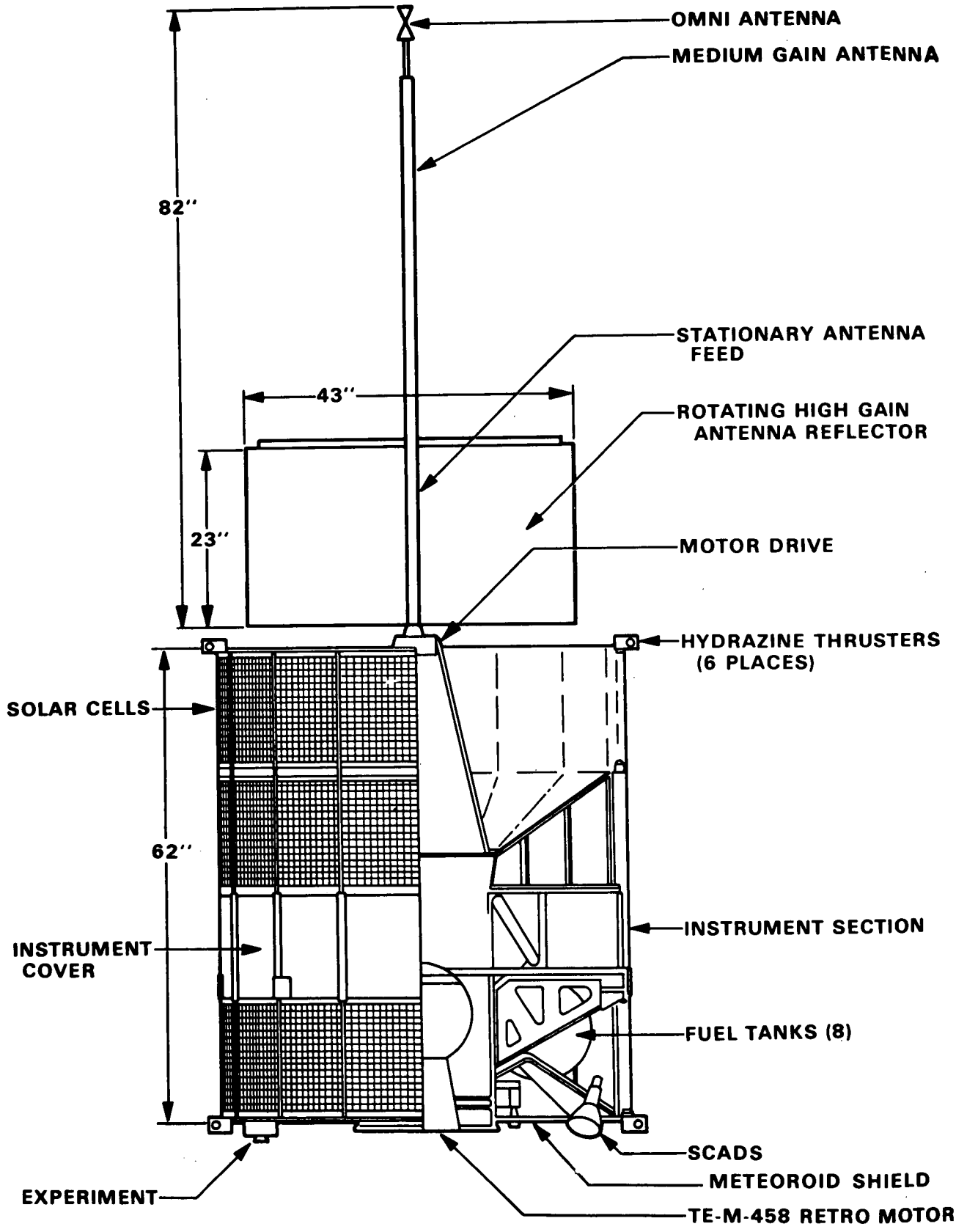

SIDE VIEW

FIGURE 4.1.3

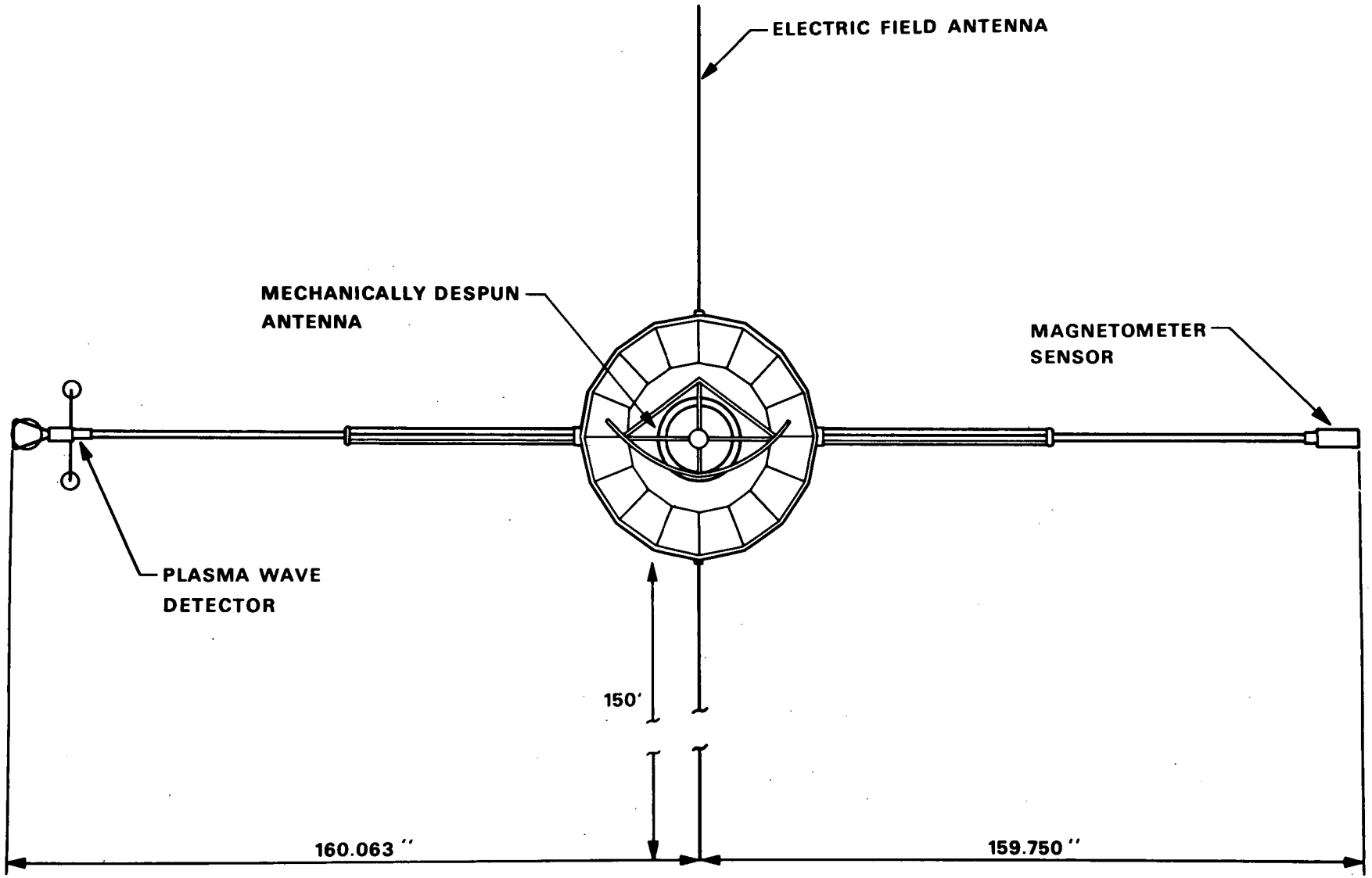
ELECTRIC FIELD ANTENNA
MECHANICALLY DESPUN ANTENNA
MAGNETOMETER SENSOR
PLASMA WAVE DETECTOR
150'
160.063"
159.750"
TOP VIEW

FIGURE 4.1.4

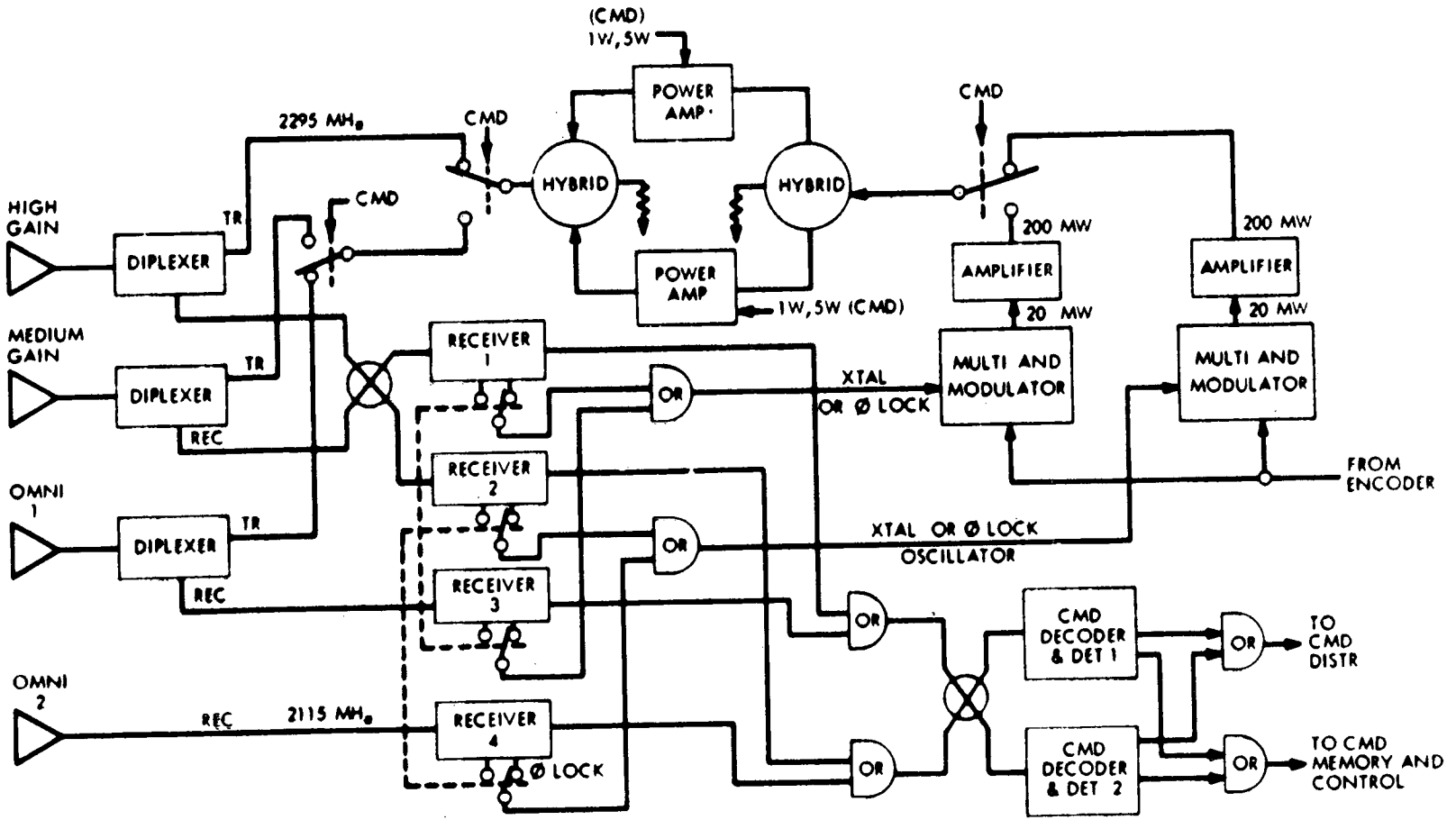

RF Subsystem, Block Diagram

FIGURE 4.2.1

The transmitter and receiver will use a combination of microwave integrated circuits (microstrip) and discrete components. Use of microstrip techniques will reduce the size and weight of resonant circuits at S-band and tend to improve unit reliability. Discrete circuit techniques will be used at lower frequencies where microstrip techniques are less effective.

The transmitter will contain a redundant pair of multiplier modulators with two-stage signal amplification. An abrupt junction diode multiplier will receive its input from the data-handling system encoder and produce a 20-milliwatt signal at 2295 MHz. Low RF power will be maintained for frequencies below S-band to reduce spurious amplitudes near the output-carrier frequency, thereby simplifying the design of the output filter. The 20-milliwatt signal will then be amplified to 200 milliwatts in a single-stage integrated microwave preamplifier. The preamplifier output will be split into two equal amplitude components and channeled to separate power amplifiers. Each power amplifier will be a two-stage microwave integrated circuit which will develop a 5-watt output.

A nominal transmitter output of 1 watt, a 5-watt output from a single power amplifier, or a 10-watt output from the combined power amplifiers will be available upon command. Three levels of power transmission will be required because the power available may be limited during some phases of the mission.

The transmitter multiplexing system will use two coaxial switches, a transfer switch, and three diplexers to switch the transmitter output to any antenna configuration selected by ground command.

Two methods will be available for deriving the transmitter frequency. During periods of noncoherent operation, when no uplink signal is present, the crystal oscillator will generate the downlink frequency. However, when an uplink signal is present, the receiver's phase-locked oscillator may be used to generate the downlink frequency. The changeover to the phase-locked mode may be accomplished by command or automatically when the receiver locks to the ground signal.

The functions of telemetry, command, and ranging will be handled on the spacecraft by an integrated transponder system as detailed in the following paragraphs.

A. Ranging: Spacecraft tracking will be aided by turn-around ranging through a coherent transponder on the spacecraft. An S-band turn-around ratio of 240/221 will be employed in the transponder, and it will be compatible with existing ground systems.

B. Transmitter: The solid state, phase modulated transmitter will be an integral part of the ranging transponder and will use the receiver VCO as a frequency source.

C. Receiver: The spacecraft receiver will be a phase-locked design in the 2025 to 2120 MHz band and will be used for both ranging and commands. Command will be PCM. The receiver VCO will also be the frequency reference for the spacecraft transmitter so that the downlink and uplink signals will be in the exact ratio of 240/221.

4.3 Antenna Subsystem

The spacecraft antenna system consists of three antennas:

- o omni antenna (OA)
- o medium gain antenna (MGA)
- o high gain antenna (HGA)

The OA with a quasi omnidirectional antenna pattern is used for transmitting and receiving during the Near-Earth-Phase, primarily before initial spacecraft attitude orientation.

The OA consists of a dipole on top of the spacecraft antenna boom and a horn on the bottom of the spacecraft, both fed through a power divider. The gain in the equatorial plane will be 0 dbi for the uplink and +0.5 dbi for the downlink. Over 80% of the spherical coverage, the gain will exceed -5 dbi.

The MGA, consisting of a collinear array, is used for transmitting and receiving. The antenna pattern (pancake shape) will be omnidirectional in the equatorial plane; the maximum deviations shall not exceed $\pm$0.5 deg. The 3 db beam-width vertical to the ecliptic plane will be 7.5 deg $\pm$ 1 deg. The polarization is linear vertical, and the gain for the uplink is 8 dbi and for the downlink is 7 dbi.

The HGA, for transmitting only, consists of a cylindrical reflector with parabolic shape, a subreflector and a slot feeder. The spot beam pattern has a 3 db beam width of 5.5 deg $\pm$ 0.5 deg in the equatorial plane and 14 deg $\pm$ 1 deg vertical to it. The polarization is linear vertical and the gain will be +23 dbi.

The reflector is mounted on the housing of a brushless DC-motor such that it remains stationary with respect to the S/C-sun line. Since the angle between S/C-sun line and S/C-earth line changes slowly but continuously during flight, the pointing with respect to the S/C-sun line can be updated semiautomatically and by ground command. The dry lubricated bearings to be used to support the motor housing have been used in a similar application before (HELIOS).

4.4 Data Handling Subsystem

A universal data system is being designed for the follow-on IMP's now called Mother-Daughter Heliocentric, and this spacecraft. The heart of the data system will be a Data Multiplex Unit (DMU), which will

be equipped with a maximum of four fixed format memories and two variable format memories capable of being loaded by ground command. The format to be telemetered is selectable by ground command. Each DMU will be capable of working at bit rates from 8 to 32, 768 bps in binary incremental steps. Tentatively it is planned to allow only three to four bit rates per spacecraft with specific values appropriate to each mission. The DMU's will be built using parts and techniques developed on IMP's and HEAO.

The DMU can be interfaced with a general purpose computer, if it is determined by the Scientific Working Team that such a computer should be available on-board.

The data rate at cometary encounter is approximately 3,000 bps based on a 10w transmitter and a 23 db high gain antenna.

4.5 Power Subsystem

The power subsystem (identical to IMP- H, I, J) uses body mounted solar panels and a silver cadmium battery for energy conversion and storage. Three rings of solar panels make up the external cylindrical surface of the spacecraft and provide approximately 140 watts of power at 28 volts during normal operation.

Regulation is provided for three different modes. When the solar array output is sufficient to support the load, a direct transfer of energy to the load occurs. As the load increases or the array output decreases, the batteries are used to support the load. When the load is less than the array capacity, the batteries are recharged. If the array output exceeds both the load and battery charge requirements, the excess is dissipated as heat in resistors appropriately located to radiate the energy away from the S/C.

The power distribution system provides 28 volts ±2 percent to the spacecraft subsystems and experiments. Converters transform this bus voltage to appropriate levels for the various electronic equipment. Table 4.4.1 outlines the power allocation.

TABLE 4.4.1

POWER ALLOCATION

Spacecraft Systems	50 watts
Transmitter	35 watts
Experiments	55 watts
TOTAL	140 watts

4.6 Structure

The IMP-H, I and J spacecraft differ from the previous IMP designs. The IMP-H structure has improvements and modifications which are based on advances in the state-of-the-art and new spacecraft requirements. Geometrically the structure is a 16-sided drum measuring 53.4 inches across flats and 62 inches in overall height. It consists of an aluminum honeycomb shelf supported by eight struts and an 18-inch diameter thrust tube on the underside. The experiment and instrument modules are mounted on the topside of the shelf. To satisfy the stringent RF and thermal requirements, the experiment and instrument section is fully enclosed by a metallic cover and side panels. Three solar array rings are used to supply power to the experiments and electronics when in orbit. Two of the rings are mounted forward and one aft of the instrument section. Appended to the exterior of the structure are two experiment booms (each approximately 10 feet long), designed to fold alongside the spacecraft at launch and to be deployed at a preselected time and sequence. The spacecraft also has two 150 foot experiment antennas (identical to IMP-J) which are deployed after separation from the launch vehicle.

The experiment and instrument modules are mounted in the instrument compartment on the top side of the honeycomb shelf. These modules are used as integral members of the structure and aid in supporting the mid-section RF shield panels. The module geometry is similar to that employed in previous IMP's but has greater depth.

The present qualified structural design of IMP-H and J will be modified for this mission. These modifications will include:

- The use of an S-band antenna system.
- The addition of increased solar cell cover glass and shielding on the aft end of the spacecraft for protection from the expected micrometeoroid flux within the cometary environment.
- A hydrazine propulsion system for trajectory adjustment and orientation
- A solid propellant retromotor to return the spacecraft to earth orbit after encounter with Grigg-Skjellerup.

4.7 Propulsion Subsystem

The design of the liquid propulsion system was enhanced by the work accomplished during the GSFC Planetary Explorer program and the current ongoing IUE (SAS-D) program. The GSFC Planetary Explorer program yielded the first design of a hydrazine (N_2H_4) velocity correction system to be utilized on a spin-stabilized spacecraft. This required that the attitude not be changed during the cruise

mode to the planet, allowing the solar array to remain normal to the sun and the electronically de-spun antenna to remain pointed at Earth. This resulted in the use of radial and/or tangential engines in conjunction with axial engines.

The system will consist of a monopropellant hydrazine propulsion subsystem to perform midcourse corrections, attitude control, and spin rate control. The selection of the body-mounted engine arrangement allows for center-of-mass excursions, plume disturbances, and solar array shadowing. The engines will be fully redundant. The propulsion system will be modular and may be preassembled, tested and mated to the spacecraft.

Ten thrusters, 5 lbs. thrust each, with Shell 405 catalytic beds will provide all trajectory correction, spin-axis precession, and spin-control capability. The tank and manifold will be modular in that the eight tanks, and the entire subsystem design will fit into the spacecraft structure and attach to it without making or breaking principal connections.

The thrusters will apply spacecraft torques as couples, with all operational modes redundant. Although minimum design firing time for all thrusters is 0.03 second, a nominal 45 degrees of spacecraft rotation (0.5 second) will be adequate.

The nominal spin rate during cruise will be 5-30 rpm. Although the spin rate is sufficient to force fuel over the outage ports, an increased spin rate during the first trajectory-correction maneuver to optimize fuel consumption is being considered.

Because of perturbations to both the spacecraft thermal and power subsystems, the spacecraft spin axis should remain perpendicular to the sun vector within a nominal ± 7 degrees during maneuvers. Precession of the spin vector about the sun line will point the thrust vector about the sun line, and a combination of axial/tangential thrusters will be used for trajectory correction. For some mission-operation sequences, the spin axis may be stabilized at this orientation after completion of the trajectory-correction maneuver; for other sequences the spin axis may be precessed to either a new or the original cruise orientation. Figure 4.6.1 shows the thruster arrangement.

Detailed thruster arrangement studies were conducted under GSFC-sponsored contracts (Ref. 1 and 2)
As more detailed information becomes available, the relative advantages of axially oriented thrusters used with radial thrusters will be analyzed and compared with the presently recommended arrangement. The velocity correction vector orientation will greatly influence the relative merits of using a combination of axial, radial, and/or tangential thrusters.

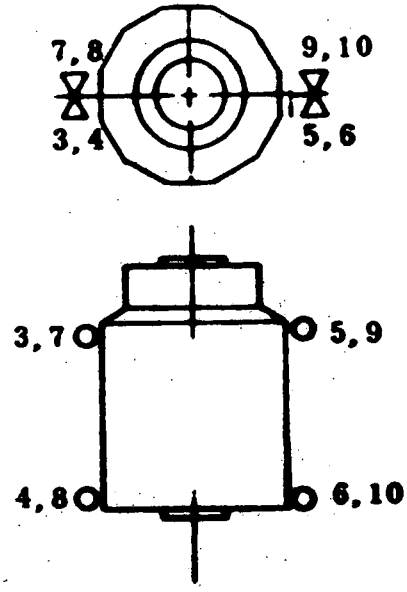

Function	Primary	Secondary
ΔV	1 - 2	3 - 5 7 - 9
ACS	3 -5 4 - 6	7 -9 8 -10
Spin	7 -5	8 - 6
-Spin	3 - 9	4 -10

FIGURE 4.6.1

Reference 1 - Planetary Explorer Liquid Propulsion Study, F. X. McKevitt, R. F. Eggers, C. W. Bolz, et al., Rocket Research Corporation June 1971 RRC-71-R-249, NAS-5-11296

Reference 2 - Planetary Explorer Liquid Propulsion Study, J. E. McCabe and V. J. Sansevero, Hamilton Standard, February 1971 SP 07R70-F

Operation

The spacecraft spin rate must be sufficient to force the fuel over the tank outage ports and to optimize propulsion system performance and maneuver accuracy. The amount of fuel required for spin control for the entire mission sequence will be minimized.

Fuel location and a sufficiently high spin rate should ensure coverage of the tank outage ports. The amount of residual fuel required to ensure outage-port coverage will depend on the level of spacecraft accelerations if solid-body rotation is assumed. The residual volume becomes very small when the spin load is greater than spacecraft accelerations by a factor of two. A worst-case factor of 10 has been assumed pending detailed study or test information regarding dynamic propellant motions. Based on this assumption a minimum spin rate of 15 rpm will be adequate.

Table 4.6.1 lists typical maneuver fuel allocations. Three hundred twenty-five (325) m/sec were allocated for the total trajectory correction maneuver. One hundred fifty (150) m/sec of which are for comet targeting corrections and the remaining 175 m/sec for earth return corrections. A total of 30 m/sec are allocated for spin and attitude correction and an additional one hundred fifty (150)m/sec for geocentric trajectory corrections and maneuvers. The total fuel allocation is 505 m/sec.

TABLE 4.6.1

MANEUVER BUDGET

	ΔV (mps)	Fuel Expenditure (lbs.)
Trajectory Corrections (Comet Targeting)	150	65.2
Spin/Attitude Corrections	15	6.3
Trajectory Corrections (Earth Return)	175	69.9
Spin/Attitude Corrections	15	5.3
Geocentric Trajectory Corrections and Maneuvers	150	50.7
Total	505	197.4

Values used in all fuel calculations are:

Isp = 215 average for trajectory corrections and spin and precession maneuvers

Rotational efficiency = 0.95 average

Moment arm = 24 inches

Nominal firing angle = 45 degrees

The blowdown ratio of 3.0 is calculated for a 13.0 inch diameter tank. Figure 4.6.2 is a schematic of the propulsion subsystem. The valve requires 14 watts to open. The maximum requirement for two tangential thrusters is an average of 3.5 watts per spin period (a 12.5 percent duty cycle). The spin velocity thrusters will require 28 watts when firing.

Use of a nutation damper to aid in the control of the spacecraft is being considered. In a preliminary arrangement, the dampers are located symmetrically in the propulsion bay. Viscous ring dampers were sized for optimum wobble Reynolds number for the cruise configuration. The diameter was restricted to 11 inches to facilitate damper packaging. The damper configuration has an 0.5-inch tube radius, contains 0.92 pound of number 200 silicone oil, and weighs 1.6 pounds. Three symmetrically arranged dampers were considered. The time constants for this damper system will be:

Spacecraft Configuration	Time Constant at 25°C
Cruise	67 minutes
After Hydrazine Depletion	90 minutes

Retromotor

A solid-propellant rocket motor will be utilized to retain the spacecraft in earth orbit after the encounter with Grigg-Skjellerup. The motor to be used has been flown successfully AIMP-D and E (Explorer 33 and 35) missions. It will impart a velocity of 200 mps.

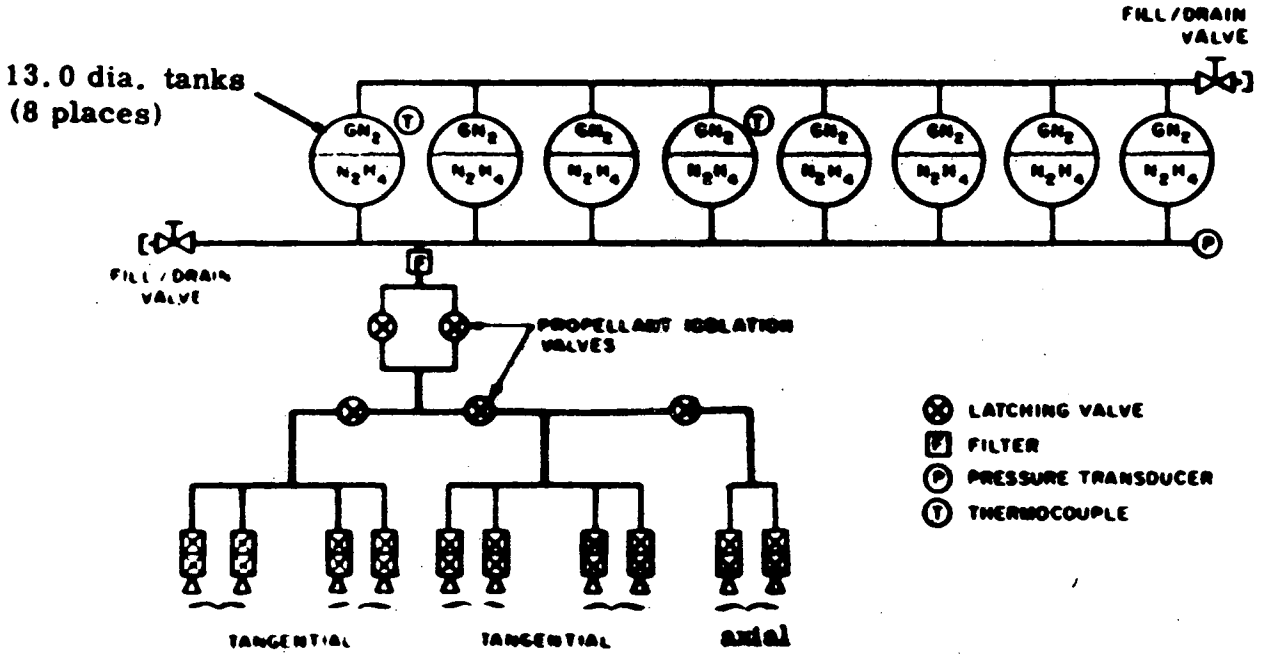

Liquid Propulsion Subsystem

FIGURE 4.6.2

Motor Case

The motor case was originally designed for the Titan vernier, and later modified for the Syncom spacecraft. It was fabricated from 17-7 PH stainless steel by marforming hemispheres made from machined blanks. The difficulty in securing marform processing for a small quantity lot, combined with the weight saving and magnetic cleanliness provided by titanium, led to the decision to fabricate the AIMP motor cases from machined titanium forgings (6AL-4V).

Propellant

The propellant for the AIMP retromotor is an ammonium perchlorate polyurethane composite with an aluminum additive, which was used in both the Titan vernier and the Syncom motors. The vacuum specific impulse of the propellant is 275 seconds. The AIMP motors were qualified between 0°F and 120°F; however this same type propellant was fired at -10°F and -30°F on other programs with slight pressure irregularities occurring at the -30°F point. Some physical and mechanical properties of the live propellant along with those of the inert propellant are listed in Table 4.6.2.

Table 4.6.2

PHYSICAL AND MECHANICAL PROPERTIES OF THE INERT AND LIVE PROPELLANTS*

Parameter	Inert	Live
Density, lb/in.^{3}	0.0616	0.0614
Specific Heat, Btu/lb°F	0.266**	0.30**
Thermal Conductivity, Btu/hr-ft-°F	0.3	0.242**
Modulus, psi	600	545
Stress, psi	100	94
Strain, in./in.	0.29	0.29

*Temperature sensitive characteristics are specified for 80°F
**These values as actually measured by Naval Propellant Plant, Indian Head, MD.

The propellant grain design for the AIMP motor is a head-end, eight-point star, the same design used on the Syncom motor. The igniters are located with their centerlines directed into the propellant vallys. Automatic ignition conditions for the propellant are 400°F for one hour, or 300°F for eight hours.

Table 4.6.3
Ballistic Performance Summary

Test Conditions	Units	Motor Serial Number					
		5	6	9	13	15	12
Motor Temperature	°F	70	70	74	75	90 to 50 grad.	50 to 90 grad.
Ambient Pressure	psia	14.7	14.7	0.05	0.05	14.7	14.7
Spin Rate	rpm	0	0	26.5	27.3	0	0
Previous Conditioning		No	No	No	No	Yes	Yes
Ambient Temperature	°F	58	67	84	87	53	45
Physical Data							
Pre-fire Weight	lb	77.79	77.78	78.83	78.98	77.43	77.38
Post Fire Weight	lb	9.00	8.96	9.39	9.65	8.56	8.59
Propellant Weight	lb	68.30	68.37	68.30	68.29	68.25	68.27
Ballistic Data							
Igniters Initiated		2	2	2	2	2	1
Maximum Ignition Pressure	psia	662	686	669	683	688	715
Ignition Delay	sec	0.040	0.025	0.024	0.022	0.022	0.030
Ignition Time	sec	0.060	0.052	0.045	0.040	0.050	0.050
Burn Time	sec	22.38	22.23	22.19	22.31	22.30	22.47
Action Time	sec	23.23	23.16	23.51	23.09	23.66	23.50
Maximum Chamber Pressure	psia	547	551	548	556	540	559
Average Chamber Pressure	psia	484	478	492	498	487	490
Maximum Ignition Thrust	lbf	841	846	1050	1067	868	876
Maximum Thrust	lbf	819	804	1014	1027	786	790
Specific Impulse at Vacuum	sec	278	275	276	276	277	275
Adjusted Total Impulse $\int Fdt$, (VAC)	lb-sec	19,016	18,782	18,853	18,833	18,958	18,770

The nozzle consists of an aft closure, throat, and exit cone. Whereas the Titan vernier separated the aft closure for thrust termination, the AIMP retromotor uses a fixed aft closure identical to that used on the Lincoln Lab motor. This closure is an aluminum machined part with an integral lip to retain the graphite throat, two tapped holes for mounting the igniters, 24 holes through which the closure is bolted to the motor case, and a large internal thread for attaching the exit cone. The nozzle assembly (consisting of the exit cone, aft closure, and a throat) is a 17 degree cone with an area expansion ratio of 41.7:1.

The motor is ignited by using redundant TE-P-462 igniter assemblies located external to the motor case, 180 degrees apart, and screwed into the after closure with an O-ring seal. The igniter consists of a case and head cap made from 302 stainless steel, a tube of propellant, a Holex number 4497 squib (a 1 ampere, 1 watt, no-fire, single bridgewire squib), a boron pellet booster charge, and a silica-phenolic nozzle throat section.

The ballistic parameters for all of the motor firings during the AIMP D and E program are summarized in Table 4.6.3.

4.8 Command Subsystem

The Command Decoder Unit (CDU) will be designed so that hardware modifications required to adapt it to different missions will be minimal (NASA/ESRO Mother/Daughter, NASA Heliocentric and the Cometary Mission).

The CDU will contain two independent and identical Pulse Code Modulation (PCM) command decoders except with separate addresses. Each decoder will contain an analog section, a digital section and a power supply. The decoders produce pulse type commands and serial data commands for control of experiments and spacecraft subsystems.

4.9 Programmer Subsystem

The spacecraft will employ a hydrazine system for maneuvering and attitude control. The system will be operated by ground control. The electronics associated with this system will use a star sensor for attitude determination in addition to the standard IMP earth-sun sensor system.

The attitude control electronics provides the timing and control functions required in the three operating attitude control modes. The control modes are selected by commands to the spacecraft. Each command is redundant.

4.10 Attitude-Determination Subsystem

The attitude-determination subsystem will consist of a star-field sensing system which will provide a highly accurate source of attitude data, and a sun-sensor system which will provide elevation and azimuth information with respect to the solar disk. The sun-sensor system will also include the spin-synchronous clock which generates a series of pulses synchronized to the spin rate.

The attitude-determination subsystem will have three primary components: the star-field sensing system with its electronics, the sun sensor, and the spin-synchronous clock electronics.

Two candidate star-sensor systems are available: the SCADS, under development at GSFC, and the MSS star sensor being developed by AVCO systems division. The star-field sensing subsystems will be redundant: they will contain two star sensors and one set of electronics. The optical axis at each sensor will be set in a direction that is the best compromise for three objectives: scanning of a large field of stars, shielding against impingement of direct sun and avoidance of obscuration by the spacecraft appendages. Considering the locations available and the various obstructions presented by the spacecraft design, an angle of 45 to 50 degrees between the optical axis of the sensor and the spin axis of the spacecraft is recommended.

The sensor must have a properly designed sunshade. Although several methods can reduce intense direct and diffuse reflections to a tolerable level, a cone shaped sunshade is recommended for this application.

4.11 Thermal Control

The basic objective of the spacecraft thermal design is to maintain component temperatures within the following design limits:

- Solid state detectors and battery: -10° to $+40^{\circ}$C
- Subsystems: -15° to $+50^{\circ}$C
- Boom-mounted components: -40° to $+60^{\circ}$ C

Further thermal design considerations include:

- Launch phase before attitude correction (which must be limited so that certain components will not exceed their temperature limits).
- Orbital conditions of full sunlight (and shadow periods up to 3 hours)
- Attitude control maintaining the spin axis normal to the solar vector
- An internal power dissipation of approximately 100 watts

The spacecraft thermal design will be passive and identical to IMP J, except for heaters on the retro-motor, specific experiments, the spacecraft battery and the hydrazine propulsion system. The design will employ selected thermal control coatings on the available external areas to meet the above objectives. Since the spacecraft has body-mounted solar cells, the only available external areas for thermal control are the 16 midsection panels (opposite the equipment facets) and the upper and lower covers. The thermal coatings on these areas will be as follows:

- o Midsection panels - an external coating pattern of black and white paints, the percentage of white on any panel depending on the power level and preferred temperature of the internal components
- o Upper cover and rear of upper solar array-multilayer insulation blanket
- o Lower cover (micrometeoroid shield) - an external coating of black paint. There will also be a multilayer insulation blanket around the hydrazine tanks and the retromotor.

Internally, to avoid large temperature gradients, power will be distributed uniformally, and all components and surfaces will be blackened. High power components will be platform-mounted and located away from temperature sensitive detectors. The excess electrical power will be dumped some distance from the internal components.

The boom-mounted components and propulsion systems will be analyzed separately and heaters utilized to maintain the temperature limits.

4.12 Spacecraft Wiring Harness

The primary consideration in wiring harness design is the suppression of conducted and radiated interference. Since the spacecraft is expected to contain a number of sensitive electromagnetic field experiments, as well as noise producing experiments and digital systems, isolation of various wiring harness elements is exceedingly important. Exceptionally sensitive or noisy leads are individually shielded. Sensitive leads are also routed in their own shielded bundle of subharness to minimize coupling. Special care in shielding and filtering is given to all harness components on the exterior of the main spacecraft structure. Cables from the experiment boom units plug directly into the outside faces of the experiment spacecraft assembly to further minimize coupling. Isolation between power currents and signal leads is usually maintained by using power converters with isolated primary and secondary windings to avoid generation of stray magnetic fields.

4.13 Meteoroid Protection

Lower Hydrazine Bay Shield

The mass and the velocity of a particle will determine the flux which is used in calculations of impacts resulting in penetration of the meteoroid shield.

The Summers and Charters equation (Ref. 1)-corrected for the target finite thickness - gives the greatest penetration depth for a given impact velocity. Use of this equation is a conservative measure. The Eq. can be written as

$$m = \frac{\ell^3 \rho^2 C_1^2}{(4.25)^3 \rho_m V^2} \qquad 4.12.1$$

where m = meteoroid mass, grams
ℓ = single sheet thickness, cm
ρ = target density, gms/cc
V = impact velocity, km/sec
C_1 = speed of sound in the target, km/sec
ρ_m = meteorid density, gms/cc

Equ. (4.12.1) gives the shield thickness that will stop a meteroid particle of mass m and density ρ_m moving with a velocity of V with respect to the shield. As a further conservative step it is assumed that all of the impacts are caused by particles arriving perpendicular to the surface.

In the spacecraft design, double-wall construction is used. Its effectiveness is incorporated in the Summers and Charters penetration equation by replacing ℓ by $\bar{\ell}$, where

$$\bar{\ell} = \frac{\ell_1 + \ell_2}{k}$$

For two plates, magnesium (on the outside) and aluminum (on the inside) separated by 1.75 inches of foam, the appropriate k factor is 0.23.

The speed of sound of the two materials has very similar values; therefore, the C_1^2 value is obtained by multiplying the values of the two materials.

The densities of the two materials are sufficiently different and two models are used to obtain the value for ρ^2.

These modifications are incorporated into the Summers and Charters equation to obtain the maximum mass of the particle that the design shield can withstand. The density of the particle is assumed to be 3 gms/cc and is traveling at 15 km/sec at impact. For the first model, the mass of the particle is 4.95×10^{-4} gms with a diameter of 680 microns: from the second model the mass is found to be 5.63×10^{-4} gms with a diameter of 710 microns.

Solar Cell Cover Glass

The solar cells, which cover the main portion of the spacecraft, require this relatively large area to perform their function of extracting energy from the sun. These large target areas will receive numerous impacts from meteoroid particles. The design of each cell's protective cover must be optimized, to maintain the required power level with the minimum weight protection necessary to maintain this power.

General Dynamics/Convair has evaluated hypervelocity impact effects on solar cells protected by 6 mil and 60 mil microsheet and fused silica covers. Seventy-five micron diameter glass-spheres (2.2 gm/cc) were fired at solar cells with velocities ranging between 12.6 km/sec (41,500 fps) and 27.4 km/sec (90,000 fps). The most significant result of this program (Ref. 2) was the large number of impacts that a solar cell could take and still function efficiently. These tests indicate that the 20 mil covers that will be used can adequately protect the solar cells for the lifetime of the mission including meteoroid impact with less than 15 percent degradation. Thus, the solar array could receive numerous impacts without suffering significant power loss.

References

1. Advanced Planetary Probe, Spin Stabilized Spacecraft for the Basic Mission, TRW Systems, Redondo Beach, California, Vol. II. 4547-6005-R0000, 1966.

2. Effects of Hypervelocity Impact on Protected Solar Cell, John A Fager, General Dynamics/Convair, AIAA Paper No. 65-289, July 26-29, 1965.

4.14 Ground Checkout Systems

The equipment used to operate and evaluate the performance of the spacecraft during integration and environmental testing is identical to IMP H, J and is provided in two major sections: (1) the spacecraft-experiment control, and (2) the spacecraft and experiment electrical support equipment. The following paragraphs describe the basic function of the two sections.

Spacecraft and Experiment Control

The computer ground system consists of a digital computer with special peripheral equipment for reception of telemetry and generation of commands. It contains all the equipment necessary to control the spacecraft and experiments via the RF command link; the system also receives, processes, displays, and evaluates data received via the RF telemetry link. Reduction and display of experiment data is made similar to that which the experimenter will use subsequent to launch to provide continuity of experiment calibration data, help in training experimenter personnel in interpreting the data they will receive in flight, and reveal any data processing problems which might be encountered during post launch operations. One ground station is located in GSFC Building 11 and may be used via coaxial cable to operate the spacecraft anywhere in the GSFC area. An additional mobile ground station is provided for backup and launch support operations.

Spacecraft and Experiment Electrical Support Equipment

The electrical support equipment is located at the spacecraft and primarily provides electrical power to simulate the output of the solar array and equipment to stimulate spacecraft and experiment sensors so that the associated flight hardware can be exercised and evaluated via the computer ground station. Each experimenter provides the equipment to stimulate his instruments. Because many experiments are synchronized to spacecraft spin, provision is made to generate control signals that are phaselocked to an artificial spin sequence. These control signals can be used to synchronize stimulus to the spin rate and thus check functions that are sensitive to spin or spin azimuth.

Ground Systems/Spacecraft Compatibility Test

A STADAN-compatible station (Network Test and Training Facility NTTF) at GSFC will ground-test the spacecraft to thoroughly investigate and determine that all specifications have been met and that the systems are compatible. Magnetic tapes with spacecraft data recorded during the tests will be processed to determine that the total ground system is compatible. The test tapes will then be duplicated and sent to the DSN and STADAN stations for readiness exercises and simulations before launch.

4.15 Tracking and Data Acquisition

The spacecraft will require support by earth-based equipment from launch through midcourse maneuvers to cometary encounter, and return to earth. Tracking and data acquisition support will consist of coordinating the resources of NASA networks and Department of Defense (DOD) launch-support facilities.

Spacecraft Communications

The spacecraft will require maintenance of communications from the earth to distances as great as 0.3 astronomical units (AU).

Table 4.14.1 shows all the NASA stations capable of supporting the mission. The notes below the table specify the assumptions used to provide a uniform criterion for comparing the potentials of the various facilities. The mission is designed to operate primarily with the 85 ft subnet.

Commands

The DSN stations will transmit commands to the spacecraft.

Data Processing

Experiment Quick-Look Data Processing

Figure 4.14.1 shows the data flow. In critical phases of the mission (postlaunch, experiment checkout, or comet encounter), GSFC will provide

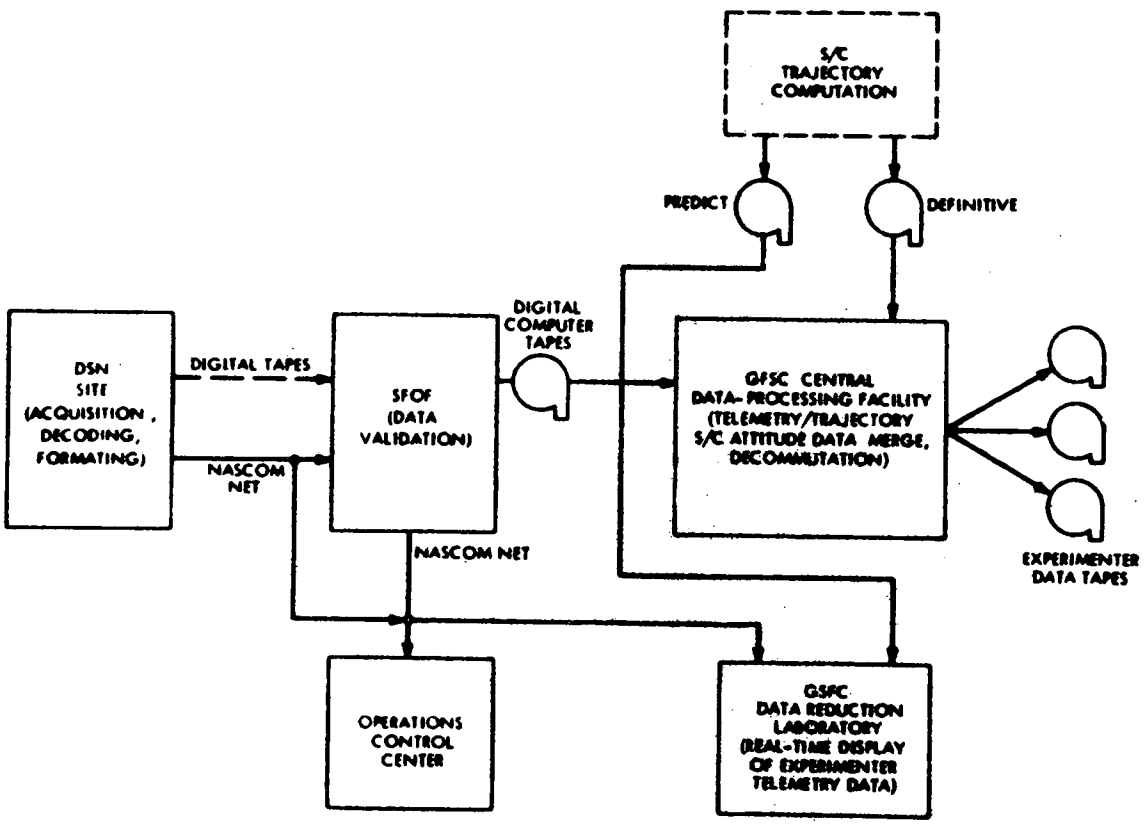

Telemetry Data Flow Diagram

FIGURE 4.14.1

near-real-time display of experimenter data. This facility, the data reduction laboratory (DRL), designed to aid the experimenter in near-real time analysis of his telemetry data, has several "user stations" connected to a Univac 1108 multiprocessor. The experimenter uses these stations, CRT displays, to communicate with the 1108 in a specially designed programming language. DRL data input is in the form of a NASCOM line from DSN and predict tapes containing spacecraft orbit and attitude data. During the cruise phase of the mission, the laboratory can be used for routine real-time verification of experiment status.

Production Data Processing

The DSN sites will acquire telemetry data from the spacecraft and perform the necessary signal detection, synchronization, sequential decoding, and formatting of the data. All telemetry data (engineering and science) will be transmitted in real time over NASCOM lines to the central data-processing facility at GSFC. Validation will consist of checking data format and comparing telemetry-system performance with standards supplied by the project. The GSFC central data-processing facility personnel will process the digital magnetic tapes by:

- Checking time continuity of all data and correcting propagation delay
- Merging telemetry, spacecraft trajectory, and attitude data on the master data tape.

In the final step, experimenter data will be decommutated on individual tapes for shipment to the experimenters. All these operations will be performed on the facility's Univac 1108 multiprocesing system. These operations are similar to those performed for other spacecraft such as the IMP series.

Inputs to the data-processing activity are validated data tapes (or equivalent NASCOM transmissions), definitive trajectory (orbit), and spacecraft-attitude tapes. The outputs are individual experimenter tapes (or equivalent data-link transmissions) and a master data tape containing merged telemetry, trajectory (orbit), and spacecraft data. The master data tape will be archived in the NASA Scientific and Technical Information Facility.

Tracking Operations

Accurate radiometric data are imperative for this mission. Position and velocity information must be known early in the cruise phase so that the proper trajectory corrections can be made to ensure a high probability of successful comet encounter. Radiometric data are available from three sources: angle information from the pointing of ground antennas, one-way and two-way Doppler measurements, and direct-range measurement. DSN will use ranging and coherent Doppler techniques to track the spacecraft and will send validated radiometric data to GSFC for real-time processing and orbit determination.

Table 4.14.1
Command Systems and Stations

Network	Antenna Diameter (ft)	Antenna Gain		Location	Uplink Frequency (MHz)	Downlink Frequency (MHz)	Transl. Ratio	Transmitter Power (kw)	Minimum Effective System Noise Temperature	Minimum Noise BW ($2B_L$) (Hz)	Maximum Range[1] Spacecraft Loop ACQ & Sstd Lock (AU)	Maximum Range[2] Command (AU)	Maximum Range[4] TM (AU)	Maximum Range[3] 6 db S/N in Minimum Carrier Loop BW (AU)	Maximum Range 6 db S/N in Loop No Modulation (AU)
		Transmit (db)	Receive (db)												
DSN	210	60.0	61.8	Calif.	2110–2120	2290–2300	221/240	20	20	10	5.8	5.8	10.1	12.4	17.5
DSN	85	51.0	53.0	Calif.	2110–2120	2290–2300	221/240	20	50	10	2.8	2.8	3.8	3.2	4.5
DSN	85	51.0	53.0	Calif.	2110–2120	2290–2300	221/240	10	20	10	1.4	1.4	3.8	3.2	4.5
DSN	85	-	-	Calif.	R&D use only at this time										
DSN	85	51.0	53.0	Central Aust.	2110–2120	2290–2300	221/240	10	65	10	1.4	1.4	3.8	3.2	4.5
DSN	85	51.0	53.0	Eastern Aust.	2110–2120	2290–2300	221/240	20	35	10	2.8	2.8	3.8	3.2	4.5
DSN	85	51.0	53.0	South Africa	2110–2120	2290–2300	221/240	10	65	10	1.4	1.4	3.8	3.2	4.5
DSN	85	51.0	53.0	Spain	2110–2120	2290–2300	221/240	20	35	10	2.8	2.8	3.8	3.2	4.5
DSN	85	51.0	53.0	Spain	2110–2120	2290–2300	221/240	10	65	10	1.4	1.4	3.8	3.2	4.5
MSFN	85	51.0	53.0	Spain	2090–2120	2270–2300	221/240	20	250	50	2.8	2.8	1.4	0.78	1.1
MSFN	85	51.0	53.0	Eastern Aust.	2090–2120	2270–2300	221/240	20	250	50	2.8	2.8	1.4	0.78	1.1
MSFN	85	51.0	53.0	Calif.	2090–2120	2270–2300	221/240	20	250	50	2.8	2.8	1.4	0.78	1.1
STADAN[3]	85	-	51.0	North Carolina	-	2200–2300	221/240	-	220	20	-	-	1.0	0.68	1.2
STADAN[3]	85	-	51.0	North Carolina	-	2200–2300	-	-	220	20	-	-	1.0	0.68	1.2
STADAN[3]	85	-	51.0	Eastern Aust.	-	2200–2300	-	-	220	20	-	-	1.0	0.68	1.2
STADAN[3]	85	-	-	Alaska	Poor visibility angle from extreme northern latitudes										

[1] 9 db S/N in S/C loop BW (20 Hz), 0 db S/C antenna gain, 75% of power in uplink carrier, S/C NF of 6 db

[2] 0 db S/C antenna gain 25% of power in modulation, S/C NF of 6 db, FSK with bit sync. 14 db Eb/No required for $P_E = 10^{-5}$ command rate of 1 per sec

[3] STADAN 85-foot-diameter antennas planned for 2200-2300-MHz receive capability by 1971. Listed parameters are estimates for these receiving capabilities

[4] 20 db S/C antenna gain 1/2 rate convolutional encoding 1.0 Jb Eb/No required for $Pe = 10^{-5}$, 10 watts transmitter on spacecraft, 25 information bits per second, PCM/PM 50% of power in modulation

[5] 20 db S/C antenna gain, 10 watts transmitter on spacecraft, 50% of power in carrier

NOTES: Additional 210-foot antennas in Spain and Australia are expected to be operational by 1973.
The assumptions used for this table provide a uniform criterion for comparing potentials of the various facilities.

Angle information, useful in the early phase of the mission, will be obtained from radars used during launch phase and from the 85-foot antennas. Angle information decreases in value as spacecraft range increases.

Doppler measurement, a powerful tool for trajectory determination, can supply most of the data needed for trajectory correction during the cruise mode, and will be the prime source of trajectory data. Although the one-way Doppler frequency shift is easy to measure, the measurement may be in error because the stability of the spacecraft oscillator is unknown after launch. A two-way Doppler measurement removes the unknown but requires the spacecraft transmitter to be phase-locked to the uplink carrier. The spacecraft command receiver, already phase-locked to the uplink carrier, can be used with a minimum of extra circuitry to serve as the frequency source for the spacecraft transmitter, producing a downlink signal phase-coherent with the uplink signal.

4.16 DETAILED WEIGHT BREAKDOWN (based on IMP-H)

Subsystem	Weight lbs.	Totals lbs.
Communications and Data Handling		68.5
S-Band Antenna	20.0	
Antenna Drive Electronics	5.0	
Encoders	16.0	
Power Converter	2.0	
Decoder and Receiver	3.3	
Transmitter (S-Band) -2	11.0	
R&RR and PCM Receiver	2.5	
PCM Decoder	1.7	
Programmers:		
System	2.0	
Experiment	2.5	
Propulsion	2.5	
Attitude Control		17.7
Sun Sensors and Electronics	2.7	
SCADS Star Sensors (2)	7.0	
SCADS electronics	2.0	
Attitude-Control Logic	1.0	
Damper	5.0	
Thermal		15.0
Power		65.8
Solar Array (w/o cover glass)	43.4	
Battery	11.2	
Shunt, Charge and Discharge Regulators	4.6	
Optical Aspect Converter	0.8	
Decoder Converter	2.3	
Encoder Converter	2.0	
Dump Resistors/Transistors	1.0	
Pyrotechnics	0.5	

Subsystem	Weight lbs.	Totals lbs.
Electrical Harness		30.0
Hydrazine Propulsion		256.8
Tanks (8)	24.0	
Engines (10)	10.0	
Fill and drain valves (3)	.9	
Pressure Transducer (2)	.6	
Isolation Valves (6)	2.5	
Filter (1)	.4	
Thermocouple (1)	.6	
Fittings and tubing	3.0	
Engine Supports (10)	3.0	
Tank Supports (8)	4.0	
Cabling	2.0	
Unusable fuel	.7	
Pressurant	2.1	
Miscellaneous	3.0	
Hydrazine Propellant (usable)	200.0	
Structure		209.3
Lower Structure Assembly	44.0	
Upper Center Tube	8.4	
Experiment Panel Support Ring	3.5	
Brackets	.7	
Harness Support Panels	2.7	
Support Columns, Experiment Panels	2.3	
Radial Braces	2.6	
Support Columns, Harness Support	2.1	
Upper Struts	1.5	
Main Structure Assembly Hardware	1.5	
Solar Panel Assemblies (3)	28.1	
R-F Antennae	1.5	
Experiment Panels	8.1	
R-F Shield Assemblies	15.3	
Bottom Shelf Assembly	1.6	
Magnetometer Boom Assembly	9.4	
Plasma Wave (TRF) Boom Assembly	9.4	
Upper Platform Assembly	2.8	
Balance Weights, etc.	30.5	
Mid Ring, Antenna Mounting	2.8	
Inertia Weights	30.5	

Subsystem	Weight lbs.	Total lbs.
Retromotor		75.3
Motor, empty	9.6	
Propellant	65.0	
Inert Consumables	.7	
Experiments		150.0
Micrometeoroid Shielding		29.4
Solar Array Cover Glass (20 mil)	12.0	
Lower Hydrazine Bay Shield	17.4	

Total Spacecraft	917.8
Vehicle Attach Fitting	22.0
Vehicle Load	939.8
Growth Contingency	32.2
Delta Capability	972.0

5.0 Schedule

A tentative schedule attempting to take into account realistic time requirements for instrument, experiment and spacecraft fabrication as well as project review and approval is presented in Figure 5.1. The general concept of the schedule is based upon the following critical milestones.

1. 15 March 1973 - Announcement of Flight Opportunity.
2. 15 June 1973 - Due date for participation in Science Working Team
3. 1 September 1973 - Selection of SWT (ground based and spacecraft experimenters)
4. 1 July 1974 - Final experiment selection and initiation of funding
5. 1 November 1975 - Prototype experiment delivery
6. 1 March 1976 - Flight unit experiment delivery
7. November 1976 - Launch
8. April 1977 - Arrival at Comet Grigg-Skjellerup

The concept of the Science Working Team has already been established in earlier programs within NASA. An additional feature of the Science Working Team for the Cometary Explorer will be the inclusion of ground based observing personnel to advise the spacecraft mission designers and experimenters with respect to the most suitable complementary observations and observing schedules. Intrinsic in this mission is the unique need for simultaneous ground based (or near earth orbiting satellite) observations of Comet Grigg-Skjellerup simultaneous with the fly-by intercept.

6 YEARS

CENTER GSFC
RESPONSIBILITY:
APPROVAL
ACCOMPLISHMENT

MILESTONE SCHEDULE

PROJECT

COMETARY EXPLORER - GRIGG/SKJELLERUP

LEVEL

ORIG. SCHED. APPR. (DATE)
LAST SCHED. CHG. (DATE) (NO.)(INITIALS)
STATUS AS OF (DATE) (INITIALS)

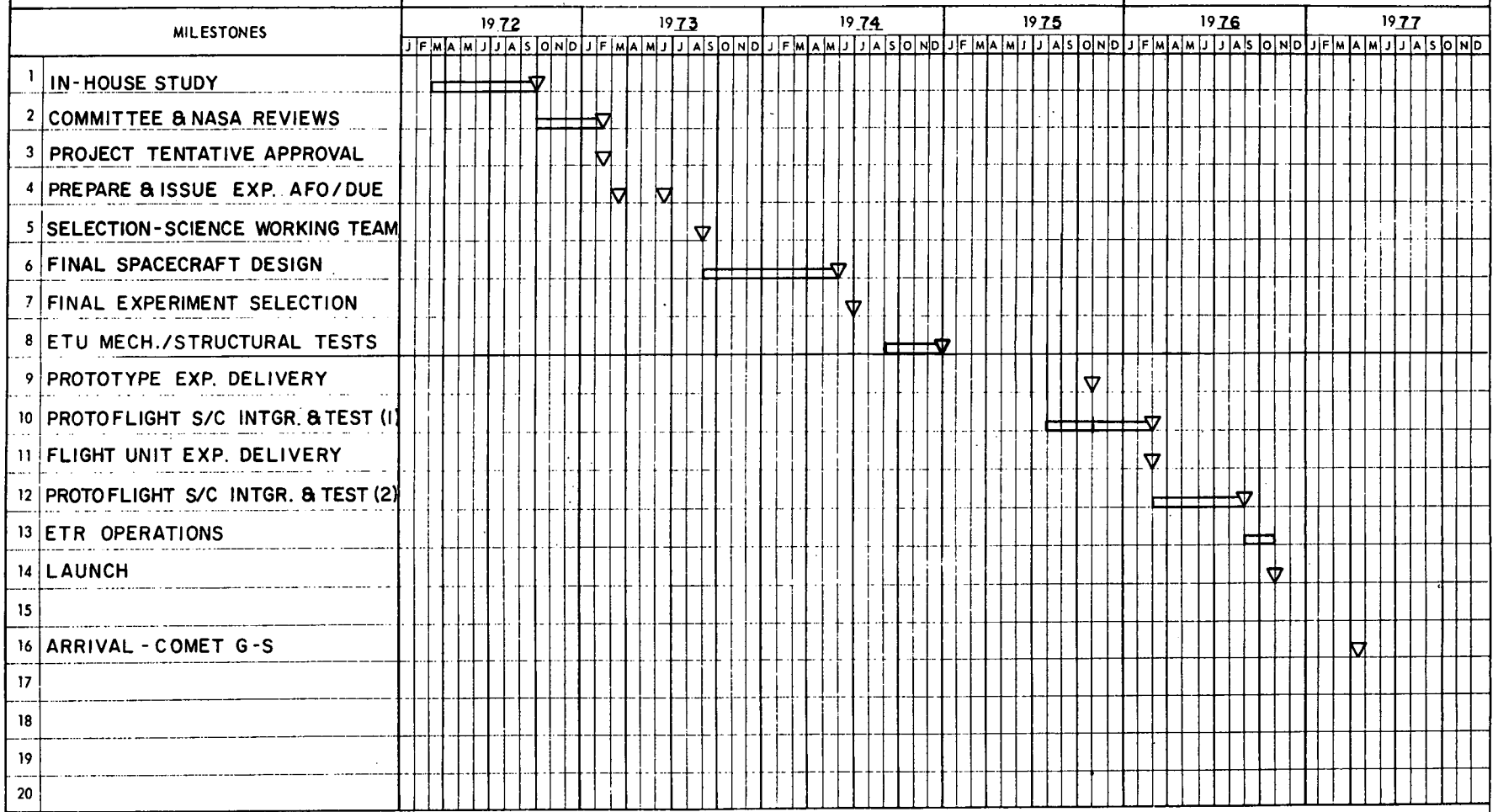

NOTES:

FIGURE 5.1

NASA Form 1304b (MAY 1966)

References

Alfven, H., Tellus 9, 92, 1957

Biermann, L. and Lust Rhea, Some New Results on the Plasma-Dynamical Processes near Comets, MPI-PAE/ASTRO 52, May 1972

Brosowski, B., and R. Wegman, Numerische Behandling eines Kometenmodells, Preprint 1972.

Comets and Asteroids: A Strategy for Exploration NASA Technical Memo TMX-64677 May 1972

Danielsson, L., in Cosmic Plasma Physics, ed., K. Schindler, 1972.

Delsemme, A. H., Review of Cometary Sciences, in the Proceedings of the Cometary Science Working Group, ed., D. L. Roberts, 1971

Friedlander, A. L., Niehoff, J. C. and Waters, J. I., Trajectory Requirements for Comet Rendezvious, Journal of Spacecraft and Rockets, Vol. 8, No. 8, August 1971.

Marsden, B. G., Catalogue of Cometary Orbits, Smithsonian Astrophysical Observatory, Cambridge, Massachusetts 1972.

1976 D'Arrest Comet Mission Study, JPL Document No. 760-66, May 10, 1971

Proceedings of the Cometary Science Working Group, Yerkes Observatory (ed. by D. L. Roberts) December 1971

Richter, N. F., The Nature of Comets, Methuen and Co., Ltd., London, 1963.

Wallis, M. K., Nature Physical Science., 233, 23, 1971

Wurm, K., the Physics of Comets, in the Moon, Meteorites, and Comets, ed. B. M. Middlehurst and G. P. Kuiper, University of Chicago Press, 1963.

* U.S. GOVERNMENT PRINTING OFFICE: 1972—735-961/18